1951

New technique for measuring photonuclear cross sections and its application to the Cu63([gamma],n)Cu62 and C12([gamma],n)C11 reactions

Lester L. Newkirk
Iowa State College

NOTE TO USERS

NEW TECHNIQUE FOR MEASURING PHOTONUCLEAR CROSS SECTIONS AND ITS APPLICATION TO THE $Cu^{63}(\gamma,n)Cu^{62}$ AND $C^{12}(\gamma,n)C^{11}$ REACTIONS

by

Lester L. Newkirk

A Dissertation Submitted to the
Graduate Faculty in Partial Fulfillment of
The Requirements for the Degree of
DOCTOR OF PHILOSOPHY

Major Subject: Applied Physics

Approved:

Signature was redacted for privacy.

In Charge of Major Work

Signature was redacted for privacy.

Head of Major Department

Signature was redacted for privacy.

Dean of Graduate College

Iowa State College

1951

TABLE OF CONTENTS

I. INTRODUCTION

Ever since Chadwick and Goldhaber (1) first demonstrated the photodisintegration of the deuteron in 1935, much work has been devoted to the study of gamma-ray induced processes. Photonuclear investigations were at first very much limited in scope. This was so because only a few monoenergetic gamma-ray sources were available, these being of insufficient energy to give rise to many reactions of interest, and of insufficient intensity, in many cases, to give strong yields. With the advent of the high energy electron accelerators (betatrons and synchrotrons) which produce photon energies up to the energy of the electrons, however, the research in this field has become quite extensive in nature.

Various lines of investigation have been followed in this field, a portion of the work being devoted to the experimental determination of photonuclear cross sections. These are of interest because of the resonance characteristics they exhibit. There have been various methods used for such determinations, and they will be discussed in the section which follows this one.

It is the purpose of this paper to describe in detail a new technique for obtaining photonuclear cross sections. The results obtained have proven to be consistent and,

once set up, the method would appear to be somewhat more convenient than other methods in existence at the present time.

Most photonuclear cross section determinations are not concerned with photons of a single energy only, but deal with photons having a continuous distribution in energy, such as are produced by a betatron or a synchrotron. Because of this, the cross section determination requires the solution of the integral equation,

$$A(E_o-\mu) = Na \int_T^{E_o-\mu} \sigma(k)\, P\,(k, E_o-\mu)\,dk. \qquad (1)$$

k = photon energy.

E_o = total electron energy.

μ = rest energy of the electron.

$E_o-\mu$ = the maximum photon energy.

T = the threshold for the reaction.

$A(E_o-\mu)$ = reaction rate.

N = number of atoms per square centimeter of sample material.

a = sample area.

$\sigma(k)$ = photonuclear cross section.

$P(k, E_o-\mu)$ = photon distribution such that $P(k, E_o-\mu)dk$ gives the number of photons per square centimeter per second (falling on the sample) which have an energy between k and $k+dk$.

A knowledge of the reaction rate and the photon distribution is obviously necessary for the determination

of the cross section. The reaction rate may be obtained experimentally by measuring the radioactivity induced in the sample and converting the result to the saturation activity. The photon distribution shape as a function of k is believed to be well known from theory (2) which has been verified experimentally at several values of $E_0 - \mu$ (3,4,5). The photon beam from a high energy accelerator may be subject to fluctuations in intensity. Also, there may be loss of some electrons in the orbit, and multiple traversals of the target by some of the electrons. Because of these factors, there must be some means for determining the relative ordinates of the respective photon distributions which are appropriate to the various electron energies at which the machine is operated while obtaining an activation curve. This means that the photon beam from the accelerator (a synchrotron was used in this experiment) must be monitored.

Ion chambers and pair spectrometers may be used to monitor the intensity of photon beams. In addition to these devices, induced radioactivity provides a monitoring method if some information is at hand concerning the photonuclear cross section of the monitor.

In the technique of cross section determination to be described in this paper, one new way of using induced radioactivity to monitor the beam is employed in a manner which appears to offer certain definite advantages. It can

be described briefly as follows. An oscillator, holding two samples of the same material, alternately slides them into the beam for a short time in such a way that while one sample is irradiated the other sample is shielded from the radiation by means of a laminated lead shield. At the same time, the electron energy of the synchrotron beam is switched alternately back and forth between two values, one of which serves as a standard for monitoring the beam intensity. This latter value remains unchanged, but the other is varied from one run to another. After allowing the oscillator to perform several complete cycles, there are two radioactive samples available. One of them, the test sample, will have been irradiated at some pre-set electron energy setting of the synchrotron; and the other, the monitor sample, will have received radiation at the monitor electron energy setting of the synchrotron. Since the monitor sample is always irradiated and counted under the same conditions, any random or long period beam intensity changes will show up in its activity. The experiment can be repeated under the very same conditions at various electron energy settings for the test sample.

The monitor sample activity of one of the runs is arbitrarily selected as the value to represent a standard of beam intensity. All test samples are then converted to the values which they would have had if the standard intensity condition had been present. This conversion is

accomplished by a simple proportion calculation. The results when plotted give an activation curve.

In order to determine the relative ordinates of the respective photon distributions, an activation curve for the reaction $Ag^{107}(\gamma,n)Ag^{106}$ was obtained with the oscillator. Since the general character of the cross section for this reaction is known, it was possible to determine the relative ordinates of the photon distributions. The results are then applicable to any activation curve taken with the oscillator.

The new technique was used to determine the relative cross sections for the reactions $Cu^{63}(\gamma,n)Cu^{62}$ and $C^{12}(\gamma,n)C^{11}$ up to 60 Mev. The results appear to be consistent and are in good agreement with other data, as a later comparison will show.

II. REVIEW OF LITERATURE

Although this thesis is concerned primarily with the experimental measurement of photonuclear cross sections, a survey of the photonuclear field in general will be presented below in order to call attention to the various aspects of the photodisintegration process.

The range of activities in this field can be broken down into cross section and related investigations, yield measurements, threshold measurements, and energy-angle distribution measurements. These various phases of photonuclear disintegration will be discussed below, with an attempt being made to follow the general historical development within each main section.

A. Cross Section and Related Investigations

The first experiments in photonuclear disintegrations following those of Chadwick and Goldhaber were made by Bothe and Gentner (6). Using the gamma-rays produced by protons on lithium and by protons on boron, they induced photodisintegration in several different nuclei, and measured and identified the resulting activities. They estimated the cross section for the $Cu^{63}(\gamma,n)Cu^{62}$ reaction to be of the order of 5×10^{-26} cm^2. Later Huber *et al.* (7) did work of a similar nature.

Hirzel and Wäffler (8), also using the gamma-rays from lithium, measured several (γ,n) cross sections (relative to the $Cu^{63}(\gamma,n)Cu^{62}$ reaction). From the data on 35 isotopes between N^{14} and Au^{195} they found a general increase of the cross section with an abrupt rise between Ca^{40} and Sc^{45}.

Russell et al. (9) obtained monochromatic gamma-ray sources of different energies by means of pile activation and have determined the (γ,n) cross sections in beryllium and deuterium at these different energies.

Nuclear emulsions and the lithium gamma-rays were used by Wäffler and Younis (10) to measure the cross sections of the $C^{12}(\gamma,n)C^{11}$ and $D^{2}(\gamma,n)p$ reactions.

The first paper on the shape of the (γ,n) cross section curve was published by Baldwin and Klaiber (11) for the $C^{12}(\gamma,n)C^{11}$ and $Cu^{63}(\gamma,n)Cu^{62}$ reactions. They determined curves of relative sample activity versus maximum energy of the 100 Mev betatron, monitoring the beam intensity with an ion chamber whose response at various energy settings of the betatron had been estimated. With the assumption of a simplified rectangular bremsstrahlung distribution, they obtained relative cross section curves by differentiating the corrected yield curves. The resulting cross section curves exhibited resonance characteristics; the curve for copper showed a sharp maximum at 22 Mev, and that for carbon showed a sharp maximum at 30 Mev with a high energy

tail.

Workers at the University of Saskatchewan (12,13,14,15), using a different technique, have measured cross section shapes for several reactions with their 26 Mev betatron and likewise have observed resonant effects. In this case the beam intensity is monitored by an r meter, imbedded in lucite, whose response to the ionization produced by the bremsstrahlung has been calculated. If the r meter response is known, and the bremsstrahlung intensity distribution is assumed to be that represented by an equation due to Schiff, then the total number of photons at each energy for a given irradiation period can be determined. With this knowledge and the activation curves corrected to the given irradiation period, it is possible to solve the integral equation for the cross section by a numerical method.

Diven and Almy (16), at the University of Illinois, have used a similar method to obtain absolute cross section curves up to 22 Mev for (γ,n) processes in Al^{27}, Ag^{107}, and Cu^{63}. Likewise, Toms and Stephens (17), monitoring the beam intensity with an ion chamber and using nuclear emulsions, have found absolute cross section curves up to 25 Mev for $Mg^{25}(\gamma,p)Na^{24}$.

Scintillation counters to detect photoprotons were used by Mann and Halpern (18) to measure the absolute cross section curves for the $C^{12}(\gamma,p)B^{11}$ reaction (up to 25 Mev).

The cloud chamber has been used by Baldwin and Klaiber (11) to observe photonuclear reactions, and by Gaertner and Yeater (19, 20) to measure single, double, and star integrated cross sections for the photodisintegration of nitrogen, carbon, helium, and oxygen by 100 Mev bremsstrahlung produced by a betatron.

Recently, a method for measuring average photon resonance energy in photonuclear reactions was devised by Koch et al. (21) and applied to the $Cu^{63}(\gamma,n)Cu^{62}$ and $C^{12}(\gamma,n)C^{11}$ processes. The absorption coefficients for the photons producing the reactions were measured in lead and aluminum. On the basis of these coefficients, and with a knowledge of the absorption-energy curves in lead and aluminum supplied by a co-worker, the average energy of the copper reaction was found to be 17.2 $\pm$ 0.4 Mev and that of the carbon reaction 22.1 $\pm$ 1.5 Mev.

Strauch (22) also has measured the effective or average photon resonance energy for several photonuclear processes by measuring in lead the absorption curve of the photons responsible for the reaction. The theory is supplied by Eyges (23) and predicts that the area under the absorption curve determines an effective or average energy of the photon causing the photonuclear reaction.

R. Sagane (24), using a technique of simultaneous activation, has measured cross section curves for several

reactions using the 70 Mev Iowa State College synchrotron. In his method the beam intensity is monitored by means of the activity induced in a monitor sample that is bombarded at the same time as the sample being studied. It is required that the photonuclear reaction in the monitor sample have a resonant energy value less than that of the reaction being studied. If this is so, and if a simplified rectangular x-ray spectrum is assumed, differentiating the corrected yield curve produces a first approximation to the cross section shape.

An experiment was done by Perlman and Friedlander (25) to determine if other competing processes, such as (γ,2n), could be responsible for the resonant shapes of the (γ,n) cross section curves. Results show, however, that in the case of Cu^{63}, as well as other nuclei, the decrease in the (γ,n) cross section in the higher energy region is not compensated for to any appreciable extent by an increase in these competing processes. On the basis of these results it seems that the photonuclear reactions are indeed due to a resonant effect.

Goldhaber and Teller (26) presented a theoretical paper in 1948 which attempted to explain photonuclear resonant phenomena. They assumed that the photons excite a dipole vibration in which all the protons in the nucleus move together in a vibratory manner always in opposition to the movement of all the neutrons. The breadth of the

resonance is assumed to be due to the transfer of energy of the orderly dipole vibration into other modes of nuclear motion. If coupling is assumed between the orderly vibratory state and these other nuclear motions, a great number of nuclear levels are obtained, each containing the dipole vibration to some extent. If the coupling is weak, however, only those levels will contain considerable contributions from the first excited state of the dipole vibration whose energy does not differ appreciably from the energy of the first excited state. As a result, a great number of nuclear levels contribute to gamma-ray absorption, but they all cluster around the first excited level. These assumptions lead to the results that the resonant energy is proportional to $A^{-1/6}$, and that the integrated cross section is proportional to A, where A is the mass number.

Steinwedel *et al.* (27) treat what they term a more plausible model which was mentioned only slightly by Goldhaber and Teller. This model assumes an interpenetrating motion of the proton fluid with density $\rho_p(r,t)$ and neutron fluid of density $\rho_n(r,t)$, under the conditions of constant total density and fixed nuclear radius, $r_0A^{1/3}$. The results indicate that the resonant energy is proportional to $A^{-1/3}$, and that the integrated cross section is just one-half that given by Goldhaber and Teller.

In another theoretical paper dealing with the resonant photonuclear effect Levinger and Bethe (28) considered dipole transitions without assuming any particular model as did Goldhaber and Teller, and Steinwedel. A function was assumed for the ground state only and a sum over all excited states was made, closure being used for the matrix elements. The results depend, therefore, only on the function assumed for the ground state. In this theory the integrated cross section equals $0.015A(1 + 0.8x)$, if $N = Z = A/2$, where N is the number of nucleons in the nucleus, Z is the atomic number, A is the mass number, and x is the fraction of attractive exchange force between a neutron and a proton. The average value of the photon energy responsible for the reaction was found to be equal to 4/3 the average kinetic energy of a nucleon in the nucleus (about 19 Mev), and is independent of A since nuclear surface effects were neglected.

B. Yield Measurements

Another type of experimental research work which has led to interesting results is that dealing with yield measurements, no attempt being made to calculate cross sections.

In 1946, Wiedenbeck (29) measured neutron yields due

to photons on beryllium by means of the neutron induced activity in rhodium. The following year Perlman and Friedlander (30) measured the relative yields of 15 (γ,n) reactions for nuclei between C^{12} and Re^{187} for 50 and 100 Mev bremsstrahlung. It was noted that the yields at both energies were essentially the same for each reaction, thus revealing for the first time that (γ,n) reactions might be of a resonance character.

In a later paper Perlman and Friedlander (25) refer to further yield measurements of not only (γ,n) reactions but also (γ,p), (γ,2n), and (γ,2p). The results show an abrupt rise in the (γ,n) yield at copper. Below copper the (γ,n) yields are approximately equal to the (γ,p) yields, but above copper (γ,n) yields are greater than (γ,p) yields. It was also stated that (γ,2n) and (γ,2p) yields were found to be much less than (γ,n) and (γ,p) respectively. Some investigation of secondary processes due to protons and neutrons was made and the results indicated that secondary processes are not responsible for any significant fraction of the yields of the primary reactions studied. It was noted that there is an abrupt rise in (γ,n) yields at A = 60. Later Perlman (31) reported, however, that additional measurements had shown that the rise in (γ,n) yields at A = 60 takes place over a range of 15 mass units and not abruptly as reported previously. A similar rise in (γ,n) yields at A = 120 also was

observed.

Wäffler and Hirzel (32) measured the ratio of the (γ,p) yield to the (γ,n) yield for several middle weight nuclei and found the ratio for many to be from 100 to 1000 times greater than expected theoretically on the statistical model. A theoretical attempt at explaining the higher proton yield was made by Schiff (33). He considered the difference in character of the compound nucleus formed by nucleon impact and that formed by gamma-ray absorption. In the latter case, the electromagnetic field of the photon varies slowly over the nucleus so that all protons are acted on by similar forces. This results in a compound nucleus that can be described by a smaller number of modes of vibration than in the case of nucleon impact. The high degree of regularity of the compound states will be reflected to some extent in the states of the residual nuclei. Under these assumptions, if the density of regular energy levels of the residual nuclei is calculated on the basis of the statistical model, the density is found to increase less rapidly with increasing excitation energy than the total level density. This results in the emission of more high energy nucleons. Due to the smaller importance of the Coulomb barrier for higher energy protons, relatively more protons will escape. A further explanation for the greater proton yield will be discussed in the section following this one.

Mock et al. (35) induced 23 (γ,n) reactions with a 20 Mev betatron and reported yield measurements. The neutron yields of 33 samples, relative to the yield of copper for lithium gamma-rays, were measured by McDaniel et al. (36). The neutrons were detected by four boron trifluoride proportional counters.

Further (γ,n) yield measurements for 18 Mev and 22 Mev bremsstrahlung were made by Price and Kerst (37) for 53 nuclei of atomic number between 22 and 83. Neutrons were detected by rhodium counters. A curve, yield=2270 $Z^{2.1}$, was fitted to the data. Baldwin and Elder (38), using essentially the same technique, measured (γ,n) yields with 50 Mev bremsstrahlung and found a curve, yield=1860 Z^2, would fit the data best.

Cameron (39) compared the photoneutron data of Price and Kerst with theoretical predictions and found that above Z equal to 30 there are experimentally more neutrons for bremsstrahlung of 22 Mev maximum energy than can be accounted for by theory from (γ,n) reactions. From theoretical considerations these neutrons can only arise from (γ,2n) and (γ,np) reactions.

Work is reported on non-fission activities produced in bismuth with photons of 48 Mev and 86 Mev bremsstrahlung (40). The results are similar to those obtained by bombardment with high energy particles in that many nucleons are emitted.

The 330 Mev synchrotron at California has been used to carry out yield measurements on 50 different nuclei by Terwilliger et al. (41). For Z greater than 30 the yield was found to be proportional to $Z^{1.7}$, where Z is the atomic number.

Scintillation counters have been applied to the study of the yields of photoprotons from 20 different nuclei (42). The relative yields increase by a factor of approximately one hundred as Z increases from 4 to 28, and then decrease to a value, at Z= 50, of about one-tenth that of the maximum at Z= 28 .

Byerly and Stephens (43) measured the yields of neutrons, protons, deuterons, and alpha particles from the photodisintegration of copper and found the yields to be respectively 3.6×10^6, 1.07×10^6, 0.34×10^6, and 0.04×10^6 particles per mole per roentgen.

C. Threshold Measurements

The first investigations dealing with this aspect of photodisintegration were carried out by Baldwin and Koch (44). Using a 22 Mev betatron they performed (γ ,n) threshold measurements on several nuclei up to Z = 47, monitoring the beam intensity with an ion chamber and observing the induced radioactivity. The activity in some cases was rather low and this, together with the fact that

the betatron was not calibrated accurately, led to somewhat large errors in the threshold measurements.

Since this first work, much additional work has been done using essentially the same technique, or one somewhat different; but in all cases the accuracy of the measurements was improved (45, 46, 47, 48, 49, 50, 51, 52). The thresholds of (γ,p) reactions have been measured also. Around the threshold, it has been found, that the yield per unit of x-ray intensity is closely proportional to the square of $(E_o-\mu)-T$, where $E_o-\mu$ is the electron energy and T is the observed threshold energy.

D. Energy-Angle Distribution Studies

It would be of interest to know something about the energy-angle distribution of the neutrons, protons, and other particles which arise from photonuclear disintegrations. Several experiments concerning such studies have been carried out.

Nuclear emulsions are well suited for this type of experiment and have been used by Toms and Stephens (53) to study the photoprotons from the $Mg^{25}(\gamma,p)Na^{24}$ reaction. A uniform angular distribution was found for all energies (up to 24 Mev), as expected on statistical theory. Diven and Almy (16) have also used nuclear emulsions to study

the energy-angle distribution of the protons from the photodisintegration of silver at 20.8 Mev and aluminum at 20.8, 17.1, and 13.9 Mev. Both silver and aluminum exhibited an isotropic distribution of protons; but in addition, silver displayed a second high energy group of protons with preference for 90° emission.

Poss (53), using the $Al^{28}(n,p)Mg^{27}$ reaction activity as a detector, also found symmetric distributions in neutrons for bismuth and tungsten, but not for lead, in contrast to the results of Price and Kerst (37) who used a rhodium counter to detect the neutrons.

Byerly and Stephens (43) in their emulsion studies of the photodisintegration of copper found that about 10 percent of the neutrons and protons which are emitted have an energy greater than expected from evaporation theory.

Levinthal and Silverman (54), using 320 Mev bremsstrahlung, studied the proton yield from carbon, copper, and lead by means of a proportional counter telescope. The results indicate that for energies less than 30 Mev an isotropic distribution results, and for energies greater than 30 Mev there is an asymmetric distribution with preference for 90° emission.

The essential features of nuclear gamma-ray absorption suggested by the above experiments are (1), a resonance excitation followed by (2), emission of a group of protons

or neutrons of low energy which in energy distribution and number fit the predictions of the statistical model and (3), an emission of a group of protons or neutrons of higher energy and angular asymmetry which falls outside the predictions of the statistical model. This additional asymmetric group of protons which is present in some reactions would help to explain the large (γ,p) to (γ,n) yield ratios found by Wäffler and Hirzel (32), referred to in the section on yield measurements.

Levinger and Bethe (56) and Courant (57) propose a picture which contains just the above features. They presume that the main process of nuclear gamma-ray absorption is the excitation of a single proton or neutron in the nucleus which occasionally escapes immediately without transferring its excitation energy to the rest of the nucleus. This results in a nuclear photo effect. In this process higher energy nucleons would be favored and would be emitted preferentially at 90° to the beam. Usually, however, the protons or neutrons interact with other nucleons and then the subsequent emission of protons or neutrons occurs in accordance with the statistical theory.

III. THEORY OF TECHNIQUE

A. Introduction

As noted previously in section I, when dealing with photons having a continuous distribution in energy as is the case here, the determination of the cross section as a function of the photon energy requires the solution of the integral equation

$$A(E_o-\mu) = Na \int_T^{E_o-\mu} \sigma(k)\, P\,(k, E_o-\mu)\,dk. \qquad (1)$$

For the definition of the different terms in this equation see section I. In order to solve this equation for the cross section, the reaction rate and the corresponding photon distribution must be known.

One way of obtaining the reaction rate would be to irradiate the sample to saturation, at which point the reaction rate is equal to the rate of decay of the radioactive nuclei. By plotting a decay curve and extrapolating back to zero time, the decay rate, i.e. the reaction rate, is obtained.

For long half-life activities it is impractical, of course, to irradiate the sample until virtually complete saturation is obtained, since this would be time consuming.

What is done instead is to irradiate the sample continuously for a time and then to determine the number of radioactive nuclei present at the end of this time. With this information, the reaction rate can be determined from the equation

$$R = A(1-e^{-\lambda t}), \qquad (2)$$

where R is the decay rate at time t, A is the reaction rate, and λ is the disintegration constant.

In the technique to be described in this paper, the sample is not irradiated continuously; but, for purposes of monitoring, the sample is placed in a device called an oscillator and alternately irradiated and shielded many times during one irradiation period. It would appear to be desirable then to show that, even under these circumstances, the reaction rate may be arrived at in a manner somewhat similar to that described above. This may be done as follows.

The irradiation situation can be represented as shown in Fig. 1, where only two and one-half cycles of the oscillator have been indicated for the sake of simplifying the analysis. Under ordinary experimental conditions, there are 40 to 50 cycles during one irradiation period. Referring to the diagram, one may write

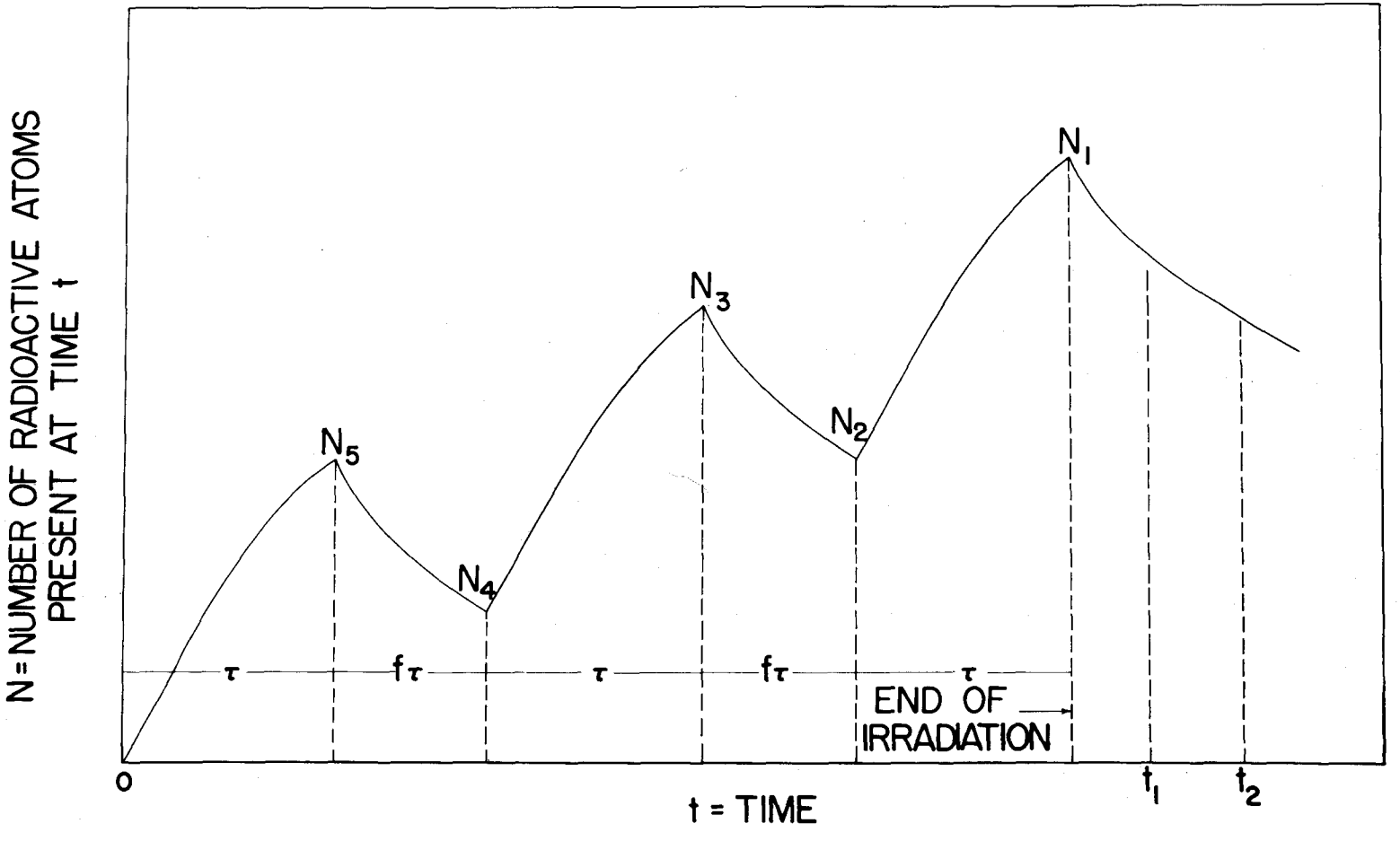

Fig. 1. Growth of radioactive nuclei under conditions of alternate irradiation and decay.

$$N_1 = N_2\, e^{-\lambda\tau} + \frac{A}{\lambda}(1-e^{-\lambda\tau}), \quad N_2 = N_3\, e^{-\lambda f\tau}, \qquad (3)$$

$$N_3 = N_4\, e^{-\lambda\tau} + \frac{A}{\lambda}(1-e^{-\lambda\tau}), \quad N_4 = N_5\, e^{-\lambda f\tau},$$

$$\text{and } N_5 = \frac{A}{\lambda}(1-e^{-\lambda\tau}).$$

In these equations A is the average reaction rate, λ is the disintegration constant of the sample, τ is the irradiation time for one cycle, and $f\tau$ the time per cycle during which the sample is shielded from the radiation.

By successive substitutions from Eqs. (3), the following expression for N_1 may be written;

$$N_1 = \frac{A}{\lambda}\left[1-e^{-\lambda\tau} + e^{-\lambda(\tau+f\tau)} - e^{-\lambda(2\tau+f\tau)} + e^{-\lambda(2\tau+2f\tau)} - e^{-\lambda(3\tau+2f\tau)}\right], \text{ or} \qquad (4)$$

$$N_1 = \frac{A}{\lambda}(1-e^{-\lambda\tau})(1+e^{-\lambda(1+f)\tau} + e^{-2\lambda(1+f)\tau}). \qquad (5)$$

$$N_1 = \frac{A}{\lambda}(1-e^{-\lambda\tau})\left[\frac{1-e^{-3\lambda(1+f)\tau}}{1-e^{-\lambda(1+f)\tau}}\right], \qquad (6)$$

since $(1+e^{-\lambda(1+f)\tau} + e^{-2\lambda(1+f)\tau})$ is a geometric progression.

$$N_1 = \frac{A}{\lambda}\left[\frac{1-e^{-\lambda\tau}}{1-e^{-(1+f)\lambda\tau}}\right](1-e^{-\lambda(T+f\tau)}), \qquad (7)$$

where $T = 3\tau + 2f\tau$ is the time from the start until the end of the run. If there are more than two cycles, Eq. (7) will still apply, and T would then represent the total time for the run in this case.

T is not necessarily small compared to unity, but if $\lambda(1 + f)\tau \ll 1$ (as it usually is), the above equation reduces to

$$N_1 = \frac{A}{\lambda} \frac{1}{1 + f} (1-e^{-\lambda T}). \qquad (8)$$

Another expression may be derived for N_1 from other considerations. The total number of disintegrations n' which occur in the time interval from t_1 to t_2 (measured from the end of the irradiation) is

$$n' = N_1 \int_{t_1}^{t_2} e^{-\lambda t}\, dt = N_1(e^{-\lambda t_1}-e^{-\lambda t_2}), \text{ or} \qquad (9)$$

$$N_1 = n'/(e^{-\lambda t_1}-e^{-\lambda t_2}) = \frac{n_o}{\eta} (e^{-\lambda t_1}-e^{-\lambda t_2})^{-1}, \qquad (10)$$

where η is the efficiency of counting, and n_o is the number of disintegrations actually obtained with a counter. Equating Eqs. (8) and (10) and solving for A gives

$$A = \frac{n_o}{\eta} \quad \frac{\lambda (1+f)}{1-e^{-\lambda T}} \left[e^{-\lambda t_1} - e^{-\lambda t_2} \right]^{-1}, \text{ or} \qquad (11)$$

$$A = n_o \; G (T, t_1, t_2, f, \eta). \qquad (12)$$

For any sample, A will be directly proportional to n_o, the counts recorded by a counter during the time interval from t_1 to t_2, providing that the time of irradiation, the time of counting, and the geometry of counting are the same for all the samples. Some variation of T (or of t_1 or t_2) from one run to another can, however, be corrected for by means of the known dependence on these parameters given by Eq. (11).

B. Method Used to Monitor the Beam Intensity

As pointed out in section I, it is necessary to provide some means for determining the relative ordinates of the respective photon spectra which are appropriate to the various electron energies at which the machine is operated while determining an activation curve. To do this requires that the synchrotron beam be monitored. This is done as follows.

A second sample, of the same material as the test sample, is alternately irradiated and shielded from the

beam at the same time as the test sample. This is accomplished by means of the oscillator discussed in section IV A. The second sample, which may be designated the monitor sample, is always irradiated at the same electron energy from one run to another, whereas the test sample is irradiated at different electron energies. For the monitor sample we may write as before

$$A_m = n_m G(T_m, t_1', t_2', f_m, \eta_m), \qquad (13)$$

where the subscript m refers to the monitor sample.

Providing that the conditions of irradiation time etc. are the same from one run to another, the number of counts from the monitor sample recorded by a counter during the period from t_1' to t_2' (measured from the end of irradiation) will indicate relative changes in the reaction rate. The relative changes in reaction rates will indicate relative changes in the beam intensity since the intensity is directly proportional to the reaction rate.

C. Application of the Results of Monitoring to the Activation Data

With a knowledge of the beam intensity changes, the activation results are then altered in the following manner.

One of the n_m, say $(n_m)_s$, is arbitrarily selected as the value to represent a standard of beam intensity. All test sample activities are then converted to the values which they would have had if the standard intensity condition had been present. This conversion is accomplished by a simple proportion.

$$\frac{n}{n_o} = \frac{(n_m)_s}{n_m}, \qquad \text{or} \qquad n = \left(\frac{n_o}{n_m}\right)(n_m)_s . \tag{14}$$

The new activation rate n is then used in place of the observed rate n_o. Since $(n_m)_s$ is a constant for each pair of samples, the activation rate to be used is directly proportional to the ratio of the test sample counts to the monitor sample counts.

D. Determination of the Adjusted Photon Distribution

Before the new activation results can be analyzed to obtain the cross section, the photon distribution must be adjusted to conform to these results.

Bethe and Heitler (2) have calculated the photon intensity distribution to be expected for electrons striking a thin target. In practice, however, most targets are not thin but are thick enough to cause scattering of the electrons to occur. Consequently, any practical

calculation involving the photon intensity distribution produced by a high energy accelerator must take electron scattering into account.

Schiff (57) has considered the energy-angle distribution from thick targets and has found that, to a good approximation, the intensity distribution at all angles is that associated with the total radiation as given by the integration of the Bethe-Heitler formula over all angles of the electron and the photon. Thus, the photon distribution falling on a sample will be essentially that given by the integrated formula of Bethe and Heitler.

Schiff also has given the following expression for the bremsstrahlung intensity distribution from a thick target in the forward direction (12).

$$\Gamma = 8\left[2(1-\gamma)(\ln\alpha - 1) + \gamma^2(\ln\alpha - \tfrac{1}{2})\right] . \qquad (15)$$

Γ = the relative intensity distribution in the forward direction.

$\gamma = k/E_0$, where k is the photon energy and E_0 is the total energy of the electron.

$$\alpha^2 = \frac{\alpha_1^2\alpha_2^2}{\alpha_1^2+\alpha_2^2}^2 \quad , \text{ where } \alpha_1 = \frac{2E_0(1-\gamma)}{\mu\gamma} \text{ and } \alpha_2 = \frac{C}{Z} = \frac{191}{Z} .$$

μ = the rest energy of the electron.

Z = the atomic number of the target material.

The distribution proposed by Schiff is shown in Fig. 2. A comparison of this distribution with that due to the integrated formula of Bethe and Heitler, both normalized to agree at 10 Mev, was made. Very good agreement was obtained

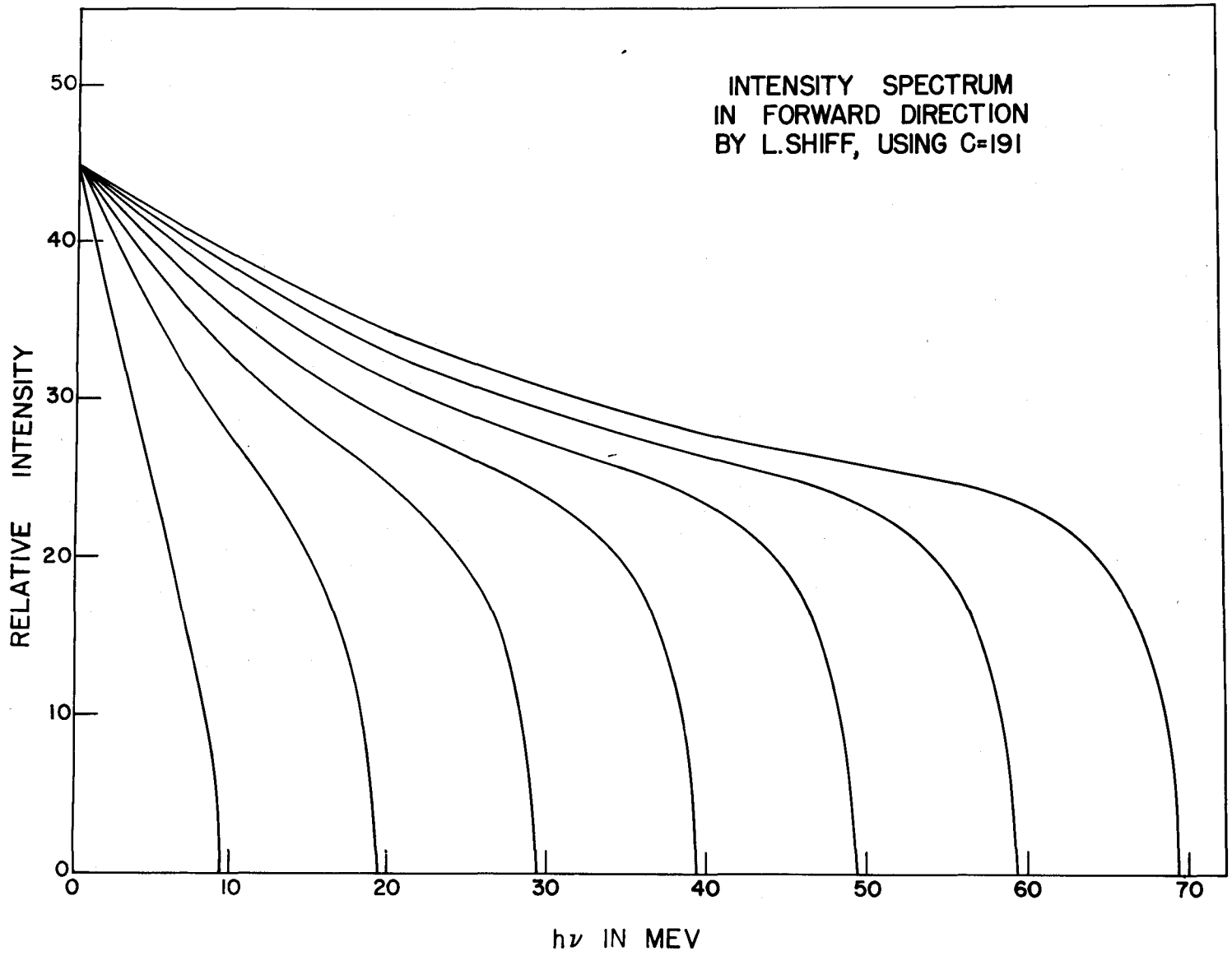

Fig. 2. Bremsstrahlung intensity distribution (relative) for electrons striking a tungsten target.

over the energy range of interest from 10 Mev to 60 Mev, the difference in areas of the two distributions for a given $E_o - \mu$ being at most about 1.5 percent. For a given $E_o - \mu$, a comparison of corresponding ordinates of the two distributions shows good agreement except at high photon energies. The maximum difference in this region is about 10 percent.

Since, as will be seen later, the cross section determination is accomplished by a numerical and graphical analysis, a family of photon distribution curves must be plotted covering the energy range of interest. It so happened that a family of Schiff photon distribution curves was available and, in view of the good agreement with the Bethe-Heitler distribution, the curves were used in the solution of the integral equation.

The spectral distortion of the photon distribution introduced by the absorption of photons in the glass walls of the synchrotron donut has been neglected since the distortion is slight, except for photons of very low energy for which it acts as a filter. This contention is supported by a comparison of two photon distribution curves shown in the paper of Katz et al. (12). For $E_o - \mu = 24.5$ Mev they calculated the effect on the photon distribution of the absorption due to the ceramic donut of their betatron. A comparison of this distribution with one which has not

been corrected for absorption, both normalized to agree at a photon energy of 10 Mev, gives agreement within 1 percent from 10 Mev to 24.5 Mev. Additional support in this matter is supplied by the work of Stokes (4), who measured the bremsstrahlung intensity distribution ($E_0 - \mu = 65$ Mev) produced by the synchrotron after passage through the donut, and found it to be in good agreement with the integrated formula of Bethe and Heitler.

It would seem that the adjusted photon distribution required is that corresponding to a constant electron intensity, multiplied by the fraction of the total photon intensity which falls on the sample. This simple interpretation, however, may be complicated by such things as the loss of electrons in the orbit, multiple traversals of the target by some of the electrons, or other factors. Because of this, the adjusted photon distribution must be determined experimentally. This is done by obtaining with the oscillator an activation curve for a reaction whose cross section is known. The reaction $Ag^{107}(\gamma, n)Ag^{106}$ was chosen, the cross section for this reaction being given by Diven and Almy (16). As will be observed below, it is preferable to use a reaction having a resonant peak value low in energy and having no appreciable high energy tail. The cross section for the silver reaction fits these considerations since it has a threshold value of 9.5 Mev, a resonant peak at about 16 Mev, and approaches zero at

around 21 Mev (see Fig. 3). In addition, the activity is easily induced making it more convenient to use than, say, the (γ,n) reaction in tantalum which, even though it has a resonant peak lower in energy (about 14 Mev), is much harder to activate.

Now the cross section curve for the silver reaction, being experimental, is somewhat in error. The adjustment of the photon distribution to the proper condition, however, will be somewhat independent of the shape of this cross section curve for those photon distribution curves whose end points lie in the energy region well above the resonant peak. The reason for this is that the photon distribution curves in this range are about the same except for a scale factor. This is especially true for photon distribution curves having high $E_o-\mu$ values, but less true for distributions having $E_o-\mu$ values around 20 Mev, the point where the Ag^{107} (γ,n)Ag^{106} cross section approaches zero.

To offset the effect of errors in the cross section on the adjustment of the photon distribution, activation results for silver were obtained only in the region from $E_o-\mu = 60$ Mev down to 19.5 Mev.

Since the general character of the cross section for the silver reaction is known, the photon distribution can be adjusted properly, resulting in a set of photon

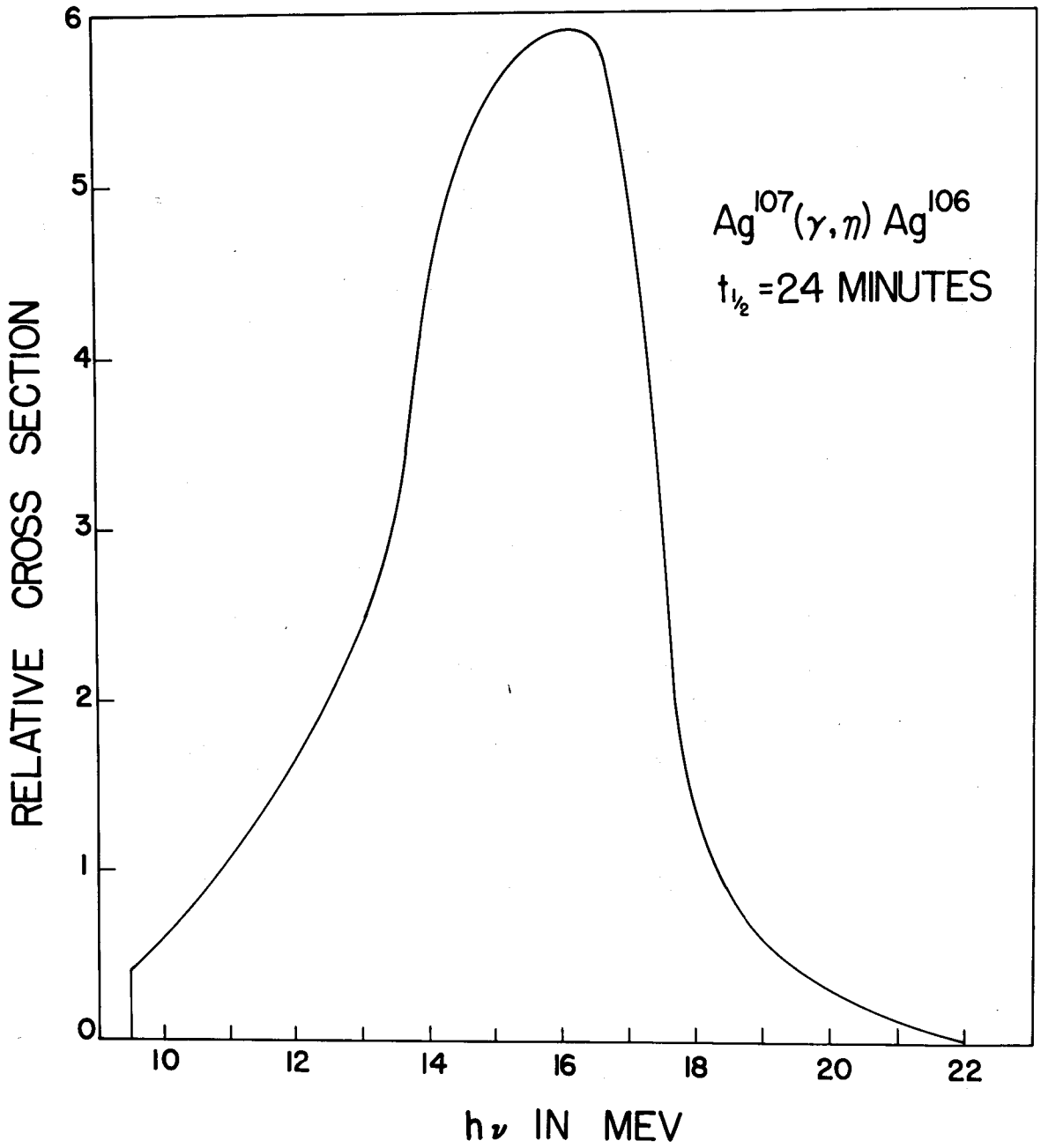

Fig. 3. $Ag^{107}(\gamma,n)Ag^{106}$ cross section (due to Diven and Almy (16)).

distribution curves which may be used to analyze any activation curve taken with the oscillator.

A plot of the relative ordinate value at 10 Mev of the normalized photon distribution is shown in Fig. 4. The threshold for the $C^{12}(\gamma,n)C^{11}$ reaction, as obtained here, is about 17.5 Mev. In order to analyze the activation curve for this reaction, therefore, it was necessary to extrapolate the curve mentioned above. The extrapolation was performed (in a straight line manner) from $E_o-\mu = 19.5$ Mev down to 12.5 Mev, however, so that the activation results for the $Cu^{63}(\gamma,n)Cu^{62}$ reaction, having a threshold of 10.6 Mev, also could be analyzed. It is believed the extrapolation is a good one since, as a later comparison will show, the results compare favorably with the results of other workers.

E. Solution of the Integral Equation

If the new activation rate n (see Eq. (14)) is used instead of the observed rate n_o, then Eq. (1) becomes

$$\frac{n_o}{n_m}\left[(n_m)_s\, G\,(T,\ t_1,\ t_2,\ f,\ \eta)\right] = Na\int_T^{E_o-\mu}\sigma(k)P(k,E_o-\mu)dk, \tag{16}$$

where the left hand factor represents the new activation results, and $P(k,E_o-\mu)$ represents the adjusted photon distribution.

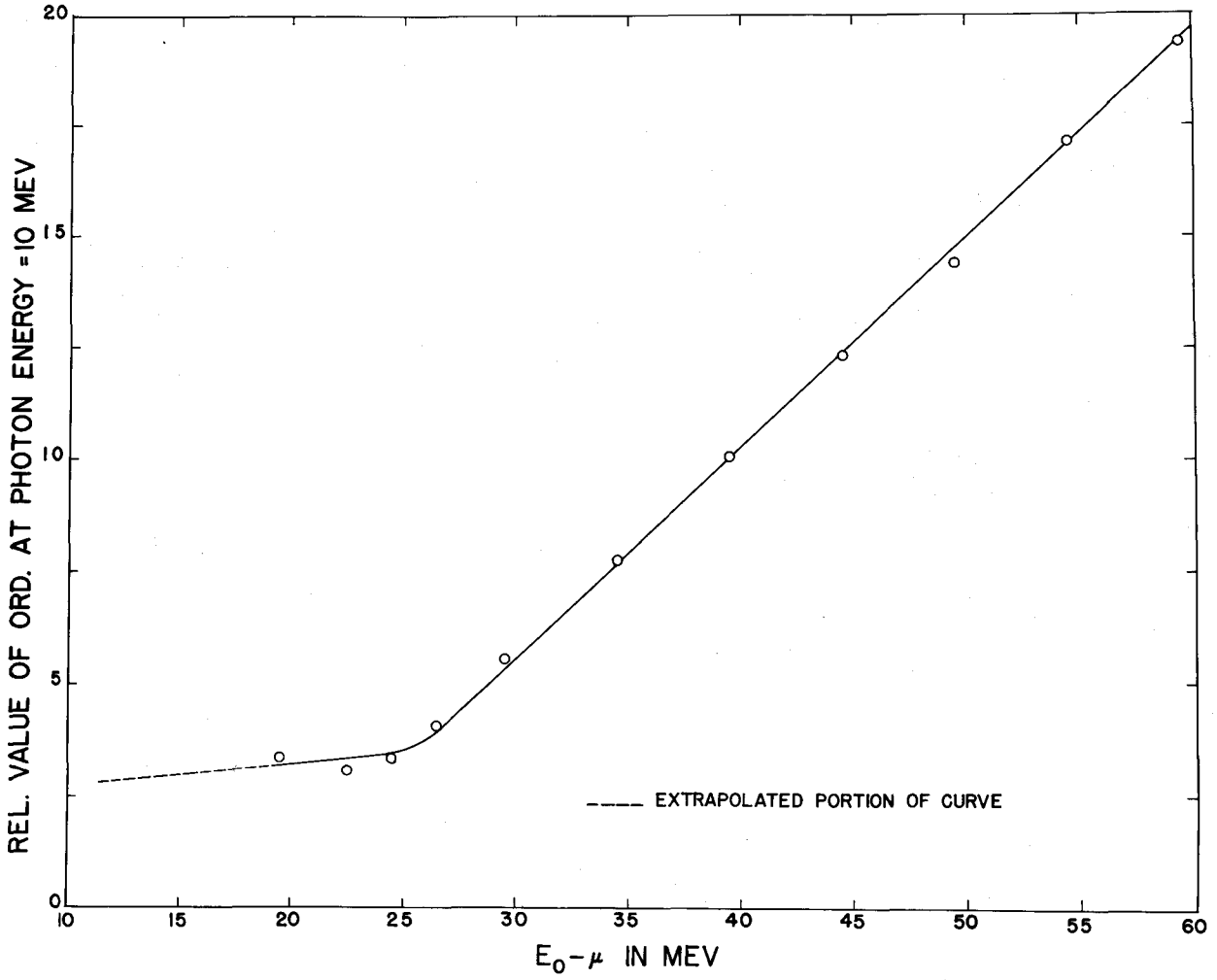

Fig. 4. Relative ordinate value at 10 Mev of the adjusted photon distribution.

A numerical way to solve this integral equation for σ (k) is to replace the integral by a summation over a series of energy intervals of width α, within each of which an average cross section is obtained.

$$\frac{n_o}{n_m}\left[(n_m)_s\, G(T,t_1,t_2,f,\eta)\right] = Na \sum_{j \geq \frac{E_o-\mu-T}{\alpha} - \frac{1}{2}}^{\infty} \sigma\left[E_o-\mu-(j+\tfrac{1}{2})\alpha\right] \qquad (17)$$

$$P\left[E_o-\mu-(j+\tfrac{1}{2})\alpha,\ E_o-\mu\right],$$

where $P\left[E_o-\mu-(j+\frac{1}{2})\alpha,\ E_o-\mu\right]$ must be expressed in units of number of photons per square centimeter per second per Mev interval, and $E_o-\mu$ must be a multiple of α. The width of the end interval must be adjusted so that it extends only from the threshold to the beginning of the next interval. The replacement of the integral by a summation leads to a set of equations in $\sigma\left[E_o-\mu-(j+\frac{1}{2})\alpha\right]$ which may be solved successively for the various $\sigma\left[E_o-\mu-(j+\frac{1}{2})\alpha\right]$. A smoothing procedure to be applied to these results will be discussed in section VI C.

Another numerical method for solving the integral equation has been developed by Katz and Cameron (58). It is based on the photon differences between successive photon distribution curves, and indirectly smooths the experimental activation curve by demanding that it have smooth first and second derivatives.

All the counting data for an activation curve may be taken under the same relative conditions from one run to another, no considerations of absolute counting being required. This means that the factor $(n_m)_s\ G(T,t_1,t_2,f,\eta)$ is a constant, and a plot of the new activation results gives a relative activation curve. Given a relative photon distribution, the solution of the integral equation will perforce give only relative values for the cross section.

If an absolute cross section curve is desired, it is necessary, after having obtained the relative cross section, to make one additional run at some value of E_o-μ using absolute methods of counting and monitoring. With these results, and with a knowledge of the relative cross section, the absolute value of the cross section for this value of E_o-μ may be calculated. Once this value is obtained, it may be applied to the relative cross section curve to convert it into an absolute one.

IV. APPARATUS

A. The Oscillator

A view of the oscillator (without its solenoid and tension spring), together with the lead shield, is shown in Fig. 5. Another picture of the oscillator in its normal operating position is shown in Fig. 6. The oscillator carries two similar samples and, when energized, alternately exposes each sample to the beam.

From Fig. 5 it is seen that the oscillator is operated in close proximity to the strong magnetic field of the synchrotron. In order to avert heating effects due to induced eddy currents, it was necessary to make the oscillator out of a non-conducting material. Therefore, the oscillator was made of 1/8 inch polystyrene sheet, its various components being glued together with acetone. It is designed to hold two thin samples ($\frac{1}{2}$ inch by $\frac{1}{2}$ inch square) in a position perpendicular to the synchrotron beam, and at a distance of about 18 inches from the synchrotron target. Sliding ways, made of bakelite and tightly fastened with brass screws to the housing of the lower magnet coil of the synchrotron, guide the oscillator in its back and forth motion. The distance of travel of the oscillator between its two extreme positions is about 5 inches.

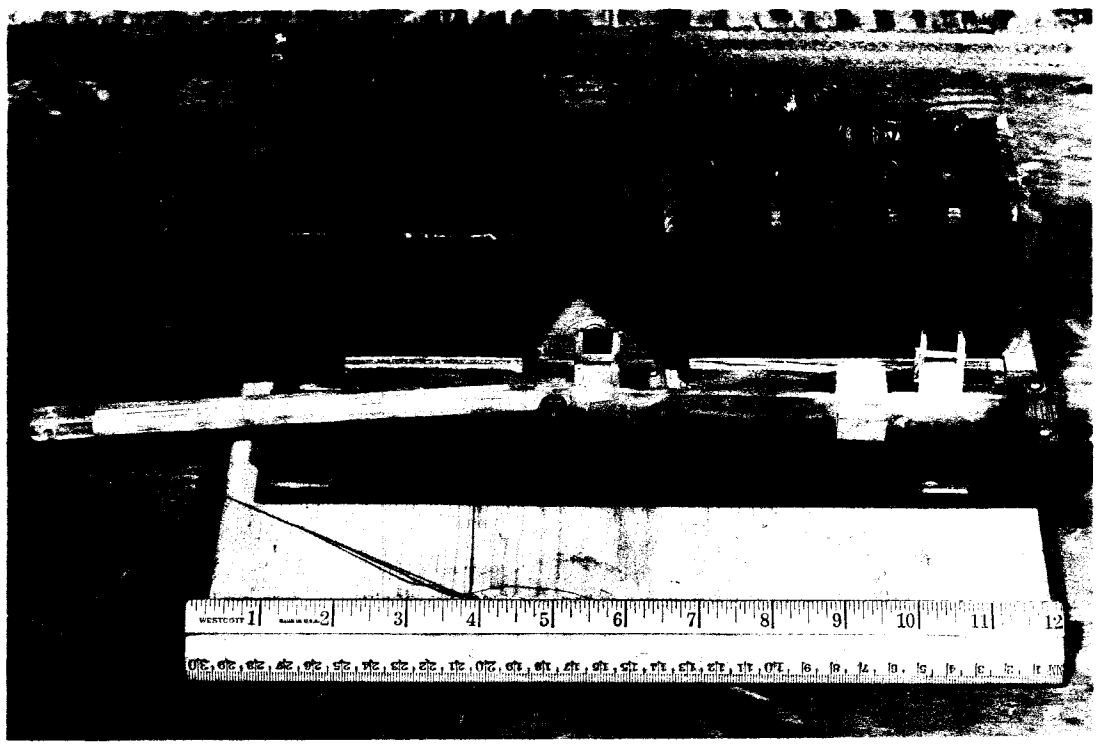

Fig. 5. View of the oscillator (without its solenoid and tension spring) and the laminated lead shield.

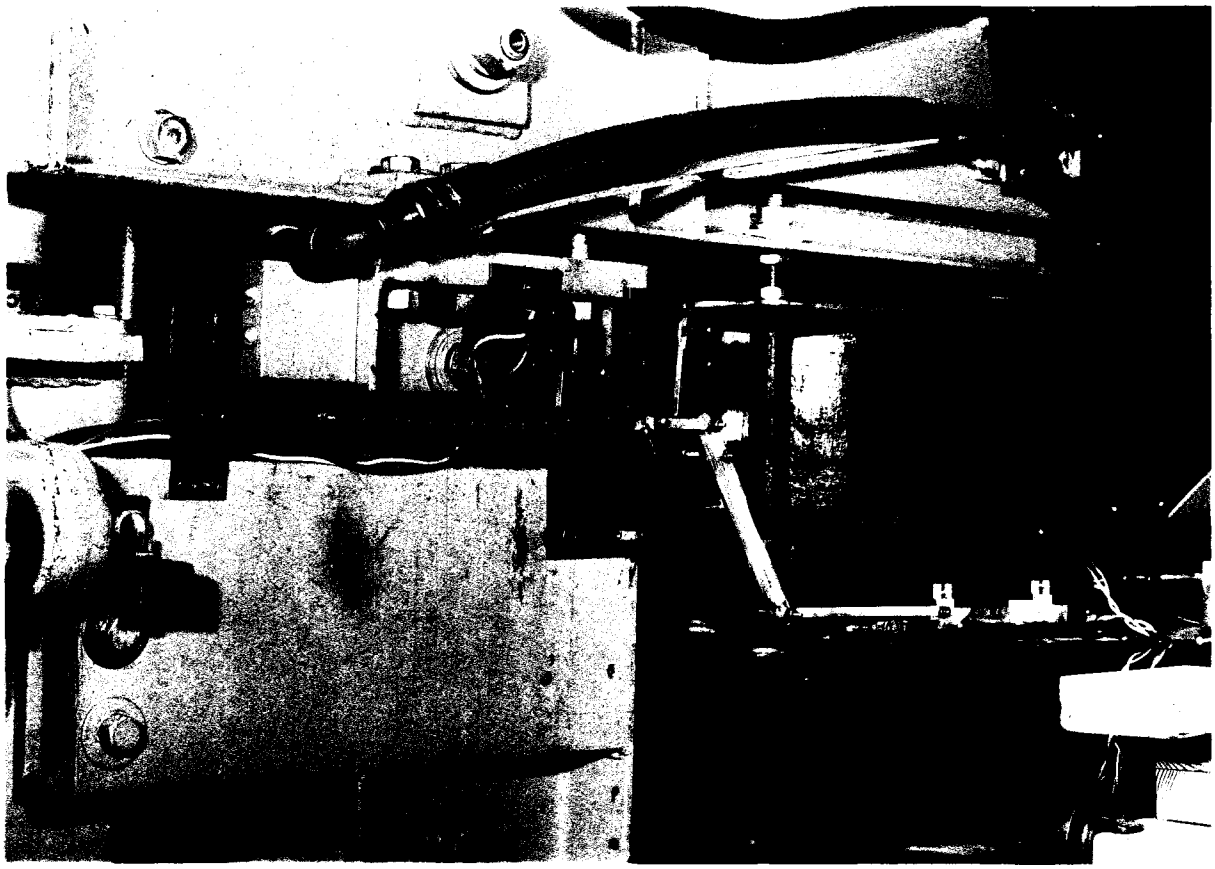

Fig. 6. View of the oscillator and lead shield in operating position between the pole pieces of the synchrotron magnet.

The oscillatory motion is provided by a solenoid which pulls the oscillator in one direction, and a tension spring which pulls the oscillator in the opposite direction when the A.C. power is removed from the solenoid.

The direction of the synchrotron beam was ascertained by means of x-ray films. The oscillator was then always aligned for each experiment so that the center of the beam passed approximately through the center of each of the two samples carried by the oscillator.

B. Timing Control Circuit for the Oscillator

A diagram of this circuit is shown in Fig. 7. One of the purposes of this unit is to apply A.C. power periodically to the solenoid which actuates the oscillator. This is accomplished by two Cramer timing devices acting together with a system of relays.

Each time the oscillator changes position, the electron energy of the synchrotron beam is switched from one value to another. This is done by changing the length of time during which the r.f. oscillator of the synchrotron remains turned on. The r.f. oscillator on period, in turn, is determined by an electronic gating circuit, whose gate length is normally controlled by a potentiometer and resistors at

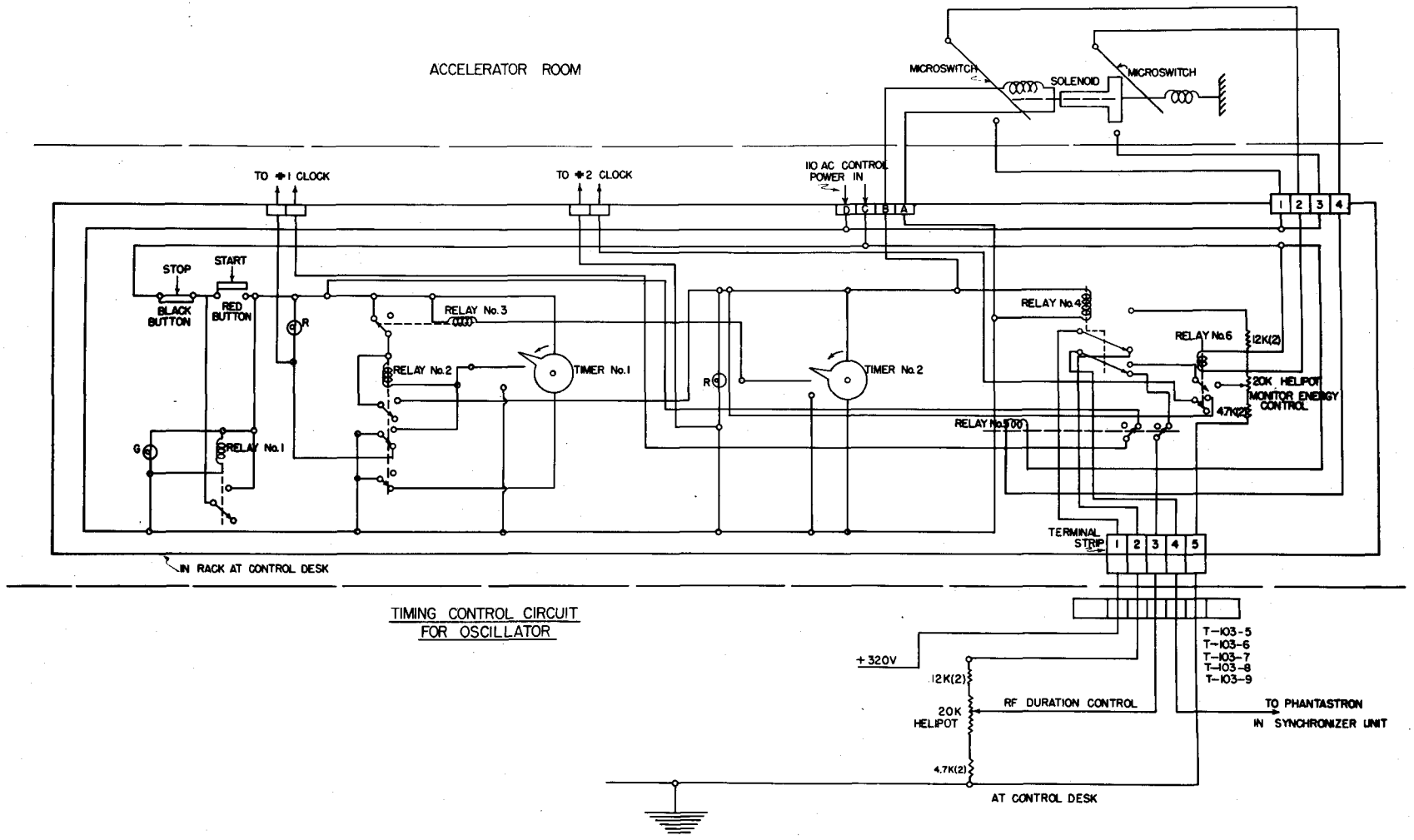

Fig. 7. Diagram of the timing control circuit of the oscillator.

the control desk. The potentiometer and resistors have been duplicated in the timing unit and the potentiometer set at a different value from the one at the control desk. A system of relays alternately switches the two potentiometer settings onto the gating circuit as the oscillator moves to and fro and, therefore, changes the energy setting of the synchrotron alternately from one value to another. Microswitches were mounted at the solenoid to cut off the synchrotron beam while the oscillator is changing position. At the end of one irradiation period many oscillations will have occurred and two radioactive samples will be available. One sample will have been irradiated at a certain electron energy setting, and the other sample will have been irradiated at a different electron energy setting.

Control knobs which control the irradiation time intervals for each of the samples are mounted on the front of the unit. The range of control is from about 1 second to 2 minutes. A record of the irradiation time for each sample is provided by two electric stop clocks which record the time to tenths of a second.

The average time during which the oscillator changes position is short, being about 0.07 seconds. This figure was estimated by operating the oscillator for a while and recording the time of operation with a stop watch. The difference between this time and that recorded by the

electric clocks divided by twice the number of complete cycles gave the average time of switching.

C. The Laminated Lead Shield

In order to shield one sample from radiation during the time the other sample is being irradiated, it was necessary to construct a lead shield. A picture of the shield, together with the oscillator, is shown in Fig. 5. The shield is about 3.5 inches high and about 4 to 5 inches thick in a dimension parallel to the synchrotron beam. It was necessary to stagger the lead sheets in both sections of the shield so as to clear certain components of the synchrotron.

Since the shield was to be used in a position between the pole pieces of the magnet in the strong magnetic field of the synchrotron, the shield had to be made of laminated lead. Therefore, 1/16 inch thick lead sheets, separated by 10 mil thick insulating cloth, were used. The lead sheets and insulating cloth are held together by means of black insulating tape. Even after several hours of use, the heating effect due to eddy currents was slight, being noticeable only in a small portion of the shield located in the strongest part of the magnetic field of the synchrotron.

A flat wooden structure to support the lead shield was

constructed (see Fig. 5). Provisions were included for securely fastening the structure to the sliding ways and to the lower coil housing of the synchrotron magnet. It was necessary to secure all the apparatus in place because the synchrotron produces considerable vibration when being operated.

The effectiveness of the shield was checked by irradiating simultaneously (at various electron energies) two copper samples arranged so that one sample was directly in the beam and the other was shielded from the beam by the lead shield. The ratio of the saturation activity of the shielded sample to the saturation activity of the unshielded sample was found to be a fraction of 1 percent.

V. METHOD OF PROCEDURE

A. Preliminary Investigations

There are apt to be other activities induced in the sample besides the one of interest. Before any activation data are taken for a particular photonuclear reaction, therefore, it is necessary to make a determination of the relative amounts of the other activities which are present. This can be done by obtaining and analyzing decay curves of the materials which are to be irradiated later for activation results.

The reactions investigated in this experiment were $Cu^{63}(\gamma,n)^{62}$, having a 10.3 minute half-life; $Ag^{107}(\gamma,n)Ag^{106}$, having a 24 minute half-life; and $C^{12}(\gamma,n)C^{11}$, having a 20.5 minute half-life. Samples of copper, silver, and polystyrene (for carbon) were irradiated for a few minutes and decay curves were then obtained.

For copper, in addition to the activity mentioned above, there was also present an activity of 12 hours half-life attributed to the $Cu^{65}(\gamma,n)Cu^{64}$ reaction. It was found, however, that the amount of this activity compared to the short lived activity is less than 1 percent if all counting is done within 20 minutes after the end of the irradiation period.

The results for silver indicated the presence of an activity of 2 minutes half-life in addition to the one referred to above. The short lived activity is due to the $Ag^{109}(\gamma,n)Ag^{108}$ reaction. In this case, if all the counting is done 18 minutes or later after the end of the irradiation period, the short lived activity will be less than 1 percent of the longer lived activity.

The decay curve for polystyrene, for which counting began 2 minutes after the end of the irradiation period, showed only the activity of 20.5 minute half-life. Thus, the counting procedure for the carbon reaction can be done any time 2 minutes or later after the end of the irradiation; but for the copper and silver reactions the limitations on counting, imposed by the results of the decay curves, must be followed.

The problem of apparent (γ,n) reactions which are actually due to (n, 2n) processes must be considered. It is believed that the neutron flux at the synchrotron is sufficiently small so that the ratio of the (n, 2n) reactions to the (γ,n) reactions is very small. This belief is supported by the work of Perlman and Friedlander (25), who found in their relative yield studies of various reactions (including the three reactions under consideration here) that the number of apparent (γ,n) processes actually due to (n, 2n) reactions was less than 1 percent of the primary (γ,n) reactions.

B. Procedure for Getting Activation Data

For testing the new technique described in this paper it was necessary only to obtain relative cross section data. Consequently, considerations of absolute monitoring and absolute counting were not required.

Several samples each of copper, silver, and polystyrene were cut into squares with $\frac{1}{2}$ inch sides so as to fit in the oscillator. The copper samples and the polystyrene samples were 45 mils thick, and the silver samples were 5 mils thick. Each sample was given a number and then weighed so that the activation results to be obtained later could be corrected for small differences in sample areas.

Data for an activation curve were taken in the following manner. Pairs of samples of the same material were placed in the oscillator and irradiated. The monitor sample always was irradiated at the same electron energy setting of the synchrotron (about 60 Mev), but the test sample was irradiated at various electron energy settings from one run to another. For each run, the irradiation periods, the times of counting, and the geometries of counting were kept the same. These conditions must be such as to give good counting rates which are neither too low nor too high. In addition, the irradiation periods should agree somewhat with the irradiation times used to obtain the decay curves, so that the extraneous activity which is

present will be only of the order of 1 percent of the total activity. Preliminary test runs were made to determine the best conditions. Usually it was found that irradiation times of around 2 or 3 minutes each for the two samples and counting periods of 4 to 5 minutes were satisfactory for the reactions investigated. After correction of the activation results for differences in sample areas and for slight differences in irradiation times, the ratio of the test sample activity to the monitor sample activity was calculated and plotted against the electron energy to give a relative activation curve.

Early in the course of the experiment it was discovered that the synchrotron beam was able to strike the samples during the time in which the oscillator was changing positions, thus introducing an error in the activation results. In an attempt to correct this difficulty micro-switches activated by the solenoid plunger were installed to turn off the synchrotron beam during the switching operations. This modification did not completely eliminate this difficulty but, for most activation results, it improved the situation to the point where the error introduced by it could be ignored. The error introduced in the monitor sample activity due to this effect was negligible in comparison to the true activity which was always rather high. The same was usually true for activities induced in the test sample, except for results obtained around the

threshold where activities were sometimes low. In this region the activity induced during the switching operation sometimes can be significant and must be considered.

This is done by making a test run with the electron energy setting of the synchrotron such that during the irradiation time for the test sample photons of sufficient energy to cause the reaction in this sample will not be created. Thus, any activity present in the test sample is that induced during the switching operation (plus the very small amount of activity present due to the ineffectiveness of the lead shield). The ratio of the test sample activity to the monitor sample activity can then be applied to the results of subsequent runs to correct them for the radiation received during the switching operation.

To meet the requirements of good counting rates over the entire activation curve, sometimes it was necessary to take data for one section of the curve under conditions different from those used to obtain the rest of the curve. The results of this section were then corrected for differences in sample weights and times of irradiation. By taking sufficient data so that the two sections overlap slightly it was possible to bring one section into smooth agreement with the adjacent section. This was done by means of a simple proportion calculation which adjusted the activation results in one section to the values which would

have resulted if they had been acquired under conditions pertaining to the adjacent section.

Relative activation data, taken in the above manner, were obtained for the $Cu^{63}(\gamma,n)Cu^{62}$ reaction, and the $C^{12}(\gamma,n)C^{11}$ reaction from their thresholds up to 60 Mev, and for the $Ag^{107}(\gamma,n)Ag^{106}$ reaction from 19.5 Mev to 60 Mev (see Figures 8, 9, and 10). It was found that data for one complete activation curve could be obtained easily in one day.

According to the theory presented in this paper, the relative activation curve for a particular reaction should be independent of the conditions of irradiation, and time and geometry of counting used. To check this, and at the same time determine the effectiveness of the technique in duplicating results, the part of the $Cu^{63}(\gamma,n)Cu^{62}$ activation curve in the region from 35 Mev to 65 Mev was obtained a second time under conditions of irradiation period, and geometry of counting different from those pertaining to the original curve. A comparison was made with the original curve and very good agreement found everywhere. The discrepancy was at most about 5 percent and usually was less than this. The discrepancy is due to statistical fluctuations in counting and to the inability to duplicate precisely conditions from one run to another. On the basis of these results, it can be stated that a few

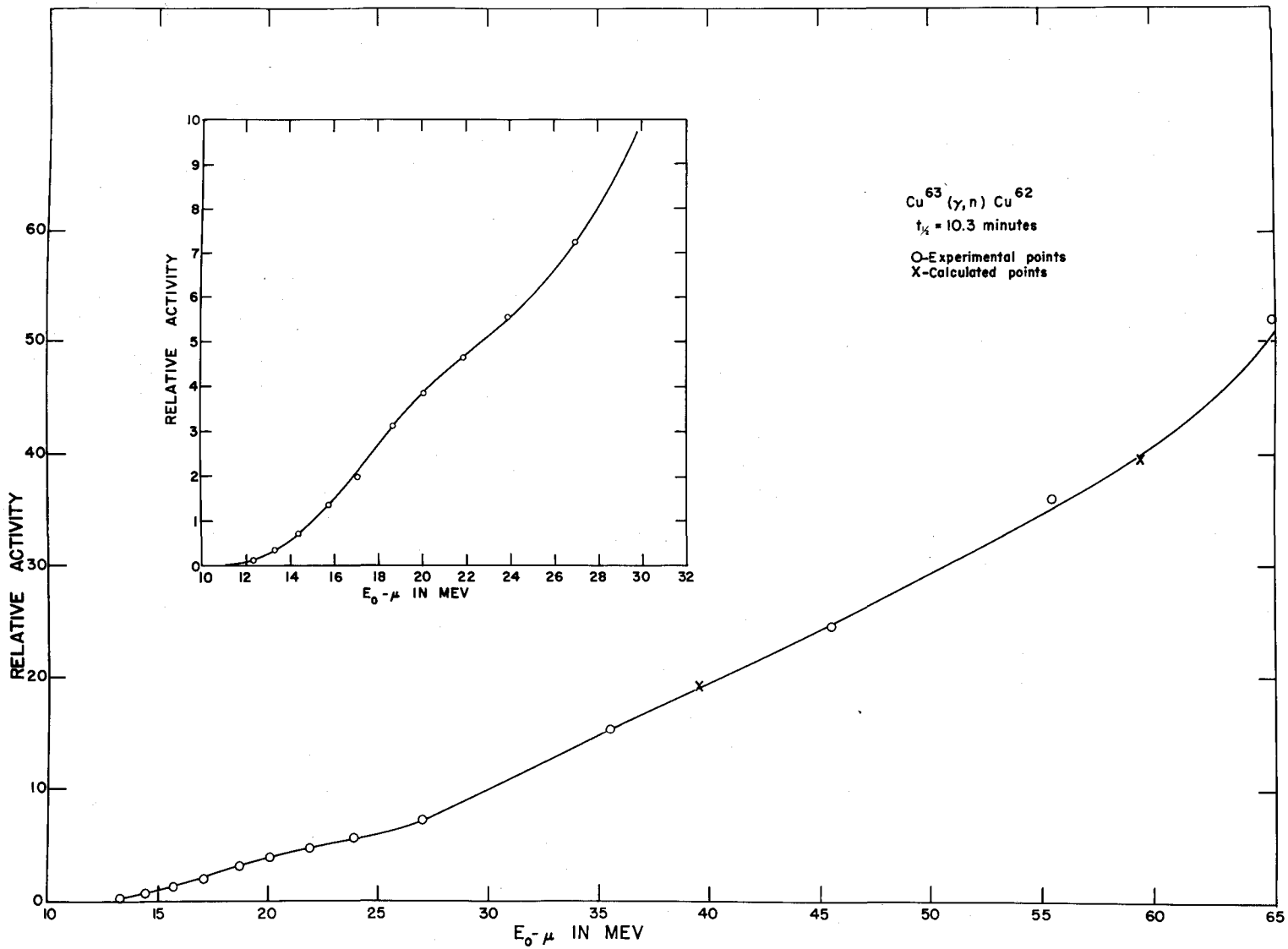

Fig. 8. $Cu^{63}(\gamma,n)Cu^{62}$ activation curve.

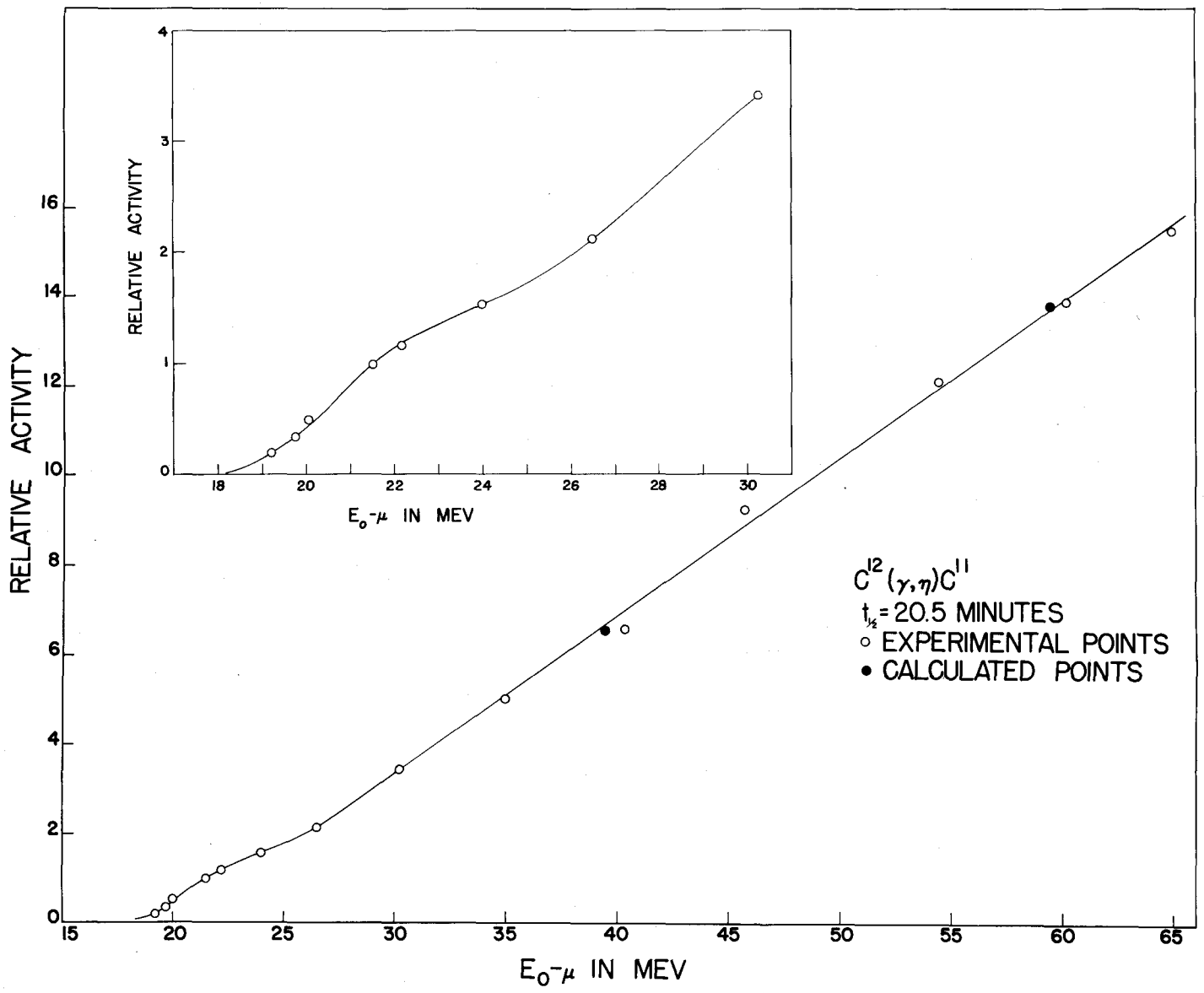

Fig. 9. $C^{12}(\gamma,n)C^{11}$ activation curve.

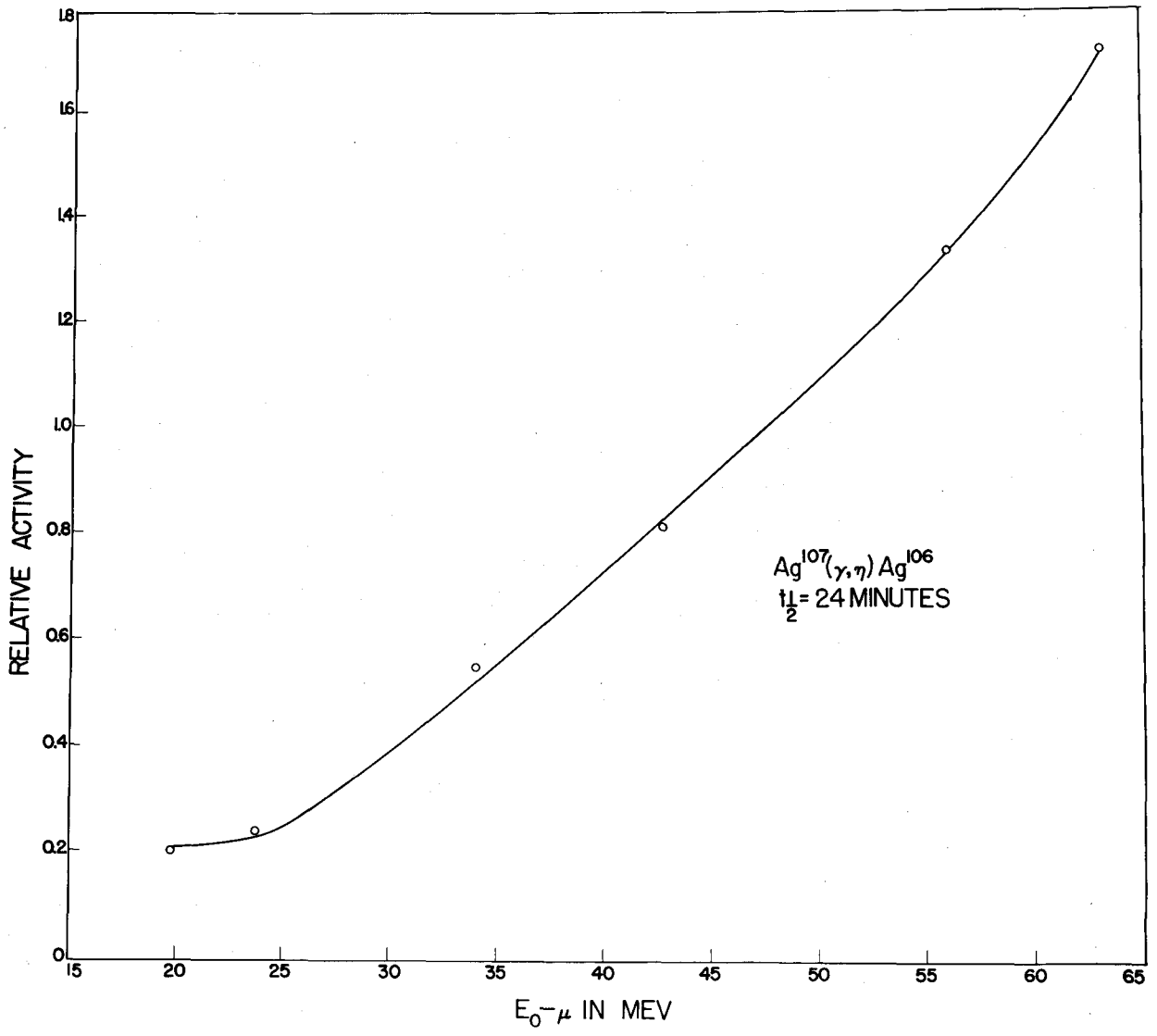

Fig. 10. $Ag^{107}(\gamma,n)Ag^{106}$ activation curve.

of the experimentally obtained activation points can be as much as 5 percent in error.

VI. RESULTS

A. Activation Data

Relative activation data for the $Cu^{63}(\gamma,n)Cu^{62}$ and $C^{12}(\gamma,n)C^{11}$ reactions were obtained from thresholds up to about 60 Mev. The results appear in Figures 8 and 9. For the reasons already mentioned in the theory, activation data for the $Ag^{107}(\gamma,n)Ag^{106}$ reaction were taken only from 19.5 Mev to about 60 Mev. The activation curve for this reaction is shown in Fig. 10.

B. Adjusted Photon Distribution

Photon distribution curves, plotted from Eq. (15) and normalized to agree at a photon energy of 17.5 Mev, were available. By means of the activation curve and the cross section curve for the $Ag^{107}(\gamma,n)Ag^{106}$ reaction, the respective photon distribution ordinates were adjusted to the values which are appropriate at the various electron energies when obtaining an activation curve. The relative ordinate values of the adjusted photon curves at a photon energy of 10 Mev were plotted against $E_0-\mu$. The resulting curve is shown in Fig. 4. The threshold for the $C^{12}(\gamma,n)C^{11}$ reaction, as obtained here, is about 17.5 Mev. As pointed

out in section III D, in order to analyze the activation curve for this reaction, it was necessary to extrapolate the adjusted photon distribution curve. The extrapolation, however, was carried out (in a straight line manner) from 19.5 Mev down to 12.5 Mev so that the activation results for the $Cu^{63}(\gamma,n)Cu^{62}$ reaction could be analyzed also. In view of the good results obtained for both reactions, it is believed that the extrapolation is a good one. Table 1 gives the values for the relative number of photons per unit area per second per indicated photon energy interval.

C. Cross Section Calculation

1. Method of calculation.

The numerical method of solution, referred to in the theory, was used to calculate the relative cross section for the $Cu^{63}(\gamma,n)Cu^{62}$ and $C^{12}(\gamma,n)C^{11}$ reactions up to a photon energy of 29.5 Mev. The photon energy interval, α, was taken to be 1 Mev.

It was pointed out in the last section that some of the activation data can be as much as 5 percent in error. Because of the nature of the calculation, each calculated cross section value is influenced not only by this error but also by the errors in all of the calculated values of

Table 1.

Relative number of photons per square centimeter per second per indicated photon energy interval.

	Photon energy interval in Mev.					
E_o-μ Mev.	10.6 -12.5	12.5 -13.5	13.5 -14.5	14.5 -15.5	15.5 -16.5	16.5 -17.5
12.5	270.0					
13.5	392.0	78.6				
14.5	444.0	139.6	65.7			
15.5	477.0	166.8	122.8	58.7		
16.5	502.0	185.6	148.0	106.4	50.5	
17.5	522.0	201.5	166.4	133.7	100.0	48.0
18.5	535.0	210.5	178.8	149.4	121.0	89.5
19.5	552.0	221.4	190.0	163.3	138.0	113.5
20.5	568.0	230.5	200.5	174.6	151.5	129.6
21.5	578.0	239.0	211.0	186.3	164.6	144.3
22.5	584.0	242.0	212.0	188.4	168.6	150.4
23.5	597.0	245.0	217.5	195.6	175.6	156.8
24.5	599.0	247.0	221.8	199.3	179.7	161.9
25.5	625.0	259.0	233.0	210.3	190.0	172.3
26.5	663.0	277.2	250.0	225.5	204.4	185.8
27.5	749.0	313.0	282.0	255.5	231.0	211.5
28.5	837.0	349.0	315.5	286.0	260.0	238.5
29.5	929.0	386.0	348.5	317.0	289.0	266.0
39.5	1794.0	752.0	687.0	628.0	575.0	528.0
59.5	3570.0	1516.0	1393.0	1278.0	1172.0	1094.0

Table 1. (Cont.)

$E_o-\mu$ Mev.	Photon energy interval in Mev. 17.5 -18.5	18.5 -19.5	19.5 -20.5	20.5 -21.5	21.5 -22.5	22.5 -23.5
12.5						
13.5						
14.5						
15.5						
16.5						
17.5						
18.5	43.6					
19.5	84.5	44.0				
20.5	105.7	79.7	37.4			
21.5	124.6	101.4	76.2	39.3		
22.5	131.1	112.6	92.8	69.8	33.4	
23.5	139.7	123.7	105.8	88.7	65.3	32.8
24.5	146.1	130.7	115.3	100.3	82.8	62.2
25.5	155.8	140.6	127.0	112.3	97.5	80.1
26.5	169.6	154.3	140.0	126.2	112.4	96.7
27.5	193.6	177.2	162.0	147.0	133.3	118.0
28.5	219.0	213.0	184.5	168.5	154.4	139.5
29.5	243.3	220.0	206.5	190.5	175.5	160.3
39.5	487.0	454.0	426.0	398.0	373.0	350.0
59.5	1018.0	949.0	893.0	837.0	788.0	742.0

Table 1. (Cont.)

	Photon energy interval in Mev.					
$E_0-\mu$ Mev.	23.5 -24.5	24.5 -25.5	25.5 -26.5	26.5 -27.5	27.5 -28.8	28.5 -29.5
12.5						
13.5						
14.5						
15.5						
16.5						
17.5						
18.5						
19.5						
20.5						
21.5						
22.5						
23.5						
24.5	31.5					
25.5	61.0	30.2				
26.5	80.8	61.7	28.2			
27.5	102.8	86.5	65.7	31.1		
28.5	124.4	109.2	91.3	69.3	32.2	
29.5	146.5	129.6	115.2	96.0	73.0	35.5
39.5	330.0	311.0	294.0	274.0	252.0	252.0
59.5	702.0	667.0	634.0	597.0	578.0	547.0

cross section which precede it. This results in errors in cross section values which can be large, since the calculation involves the difference of two numbers of about the same magnitude. Approximate values can be calculated, however, and progressive smoothing used to obtain a smooth curve. The calculation of a negative value for cross section at high energy values means that some of the previous estimated cross section values were too large.

2. $Cu^{63}(\gamma,n)Cu^{62}$ cross section results.

The threshold for this reaction was found to be 10.6 Mev, in good agreement with the value of 10.9 ± 0.2 Mev given by McElhinney et al. (40). The cross section curve was found to have a maximum value at 17 Mev, and to approach zero at around 29 Mev (see Fig. 11). For a comparison with other results see Table 2.

To determine if the cross section curve as obtained here is consistent with activation results at higher energies, the cross section values were substituted into the summation formula for the activity, and activation results calculated for $E_0 - \mu = 39.5$ Mev and 59.5 Mev. The results are plotted on the activation curve for $Cu^{63}(\gamma,n)Cu^{62}$ (see Fig. 8) and are in very good agreement with the experimental results.

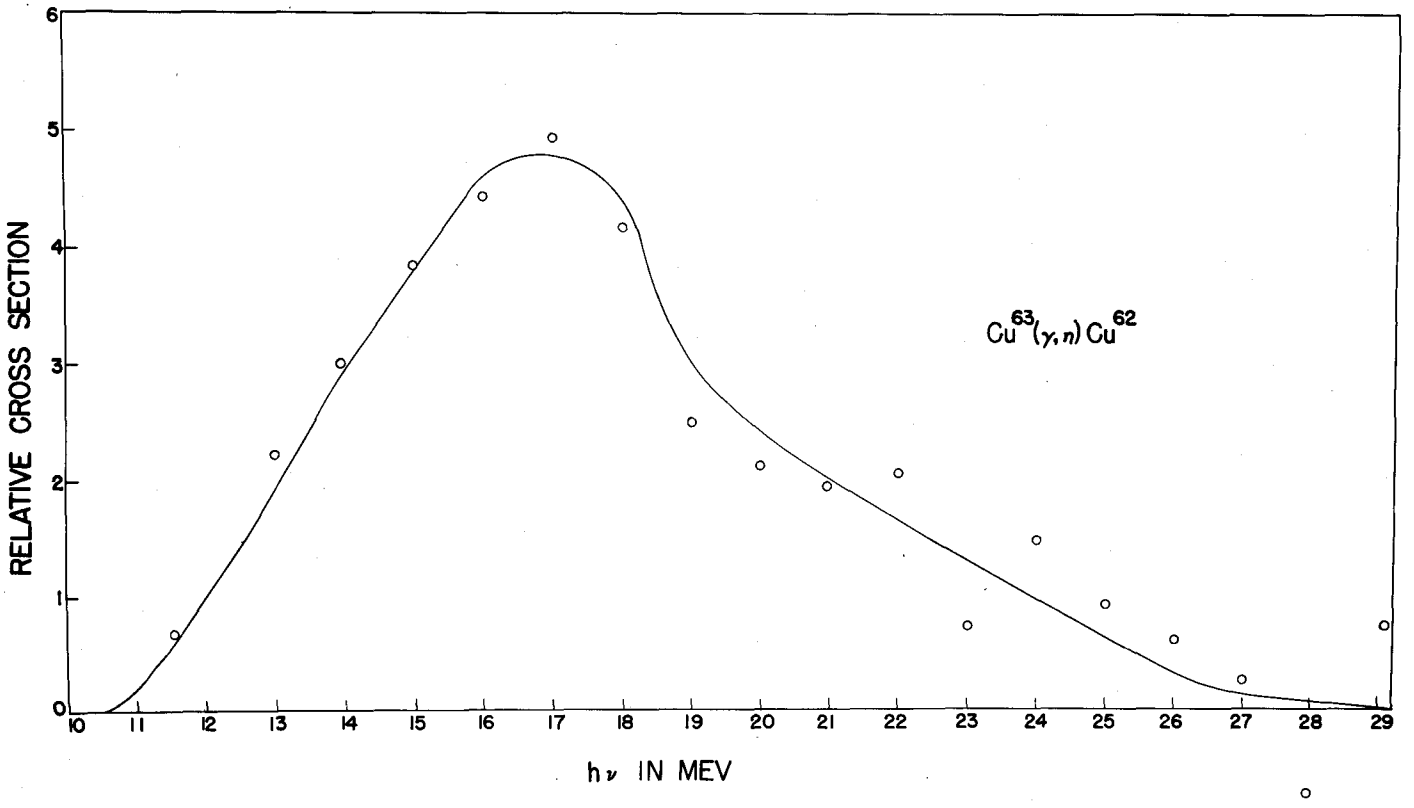

Fig. 11. Relative cross section for the $Cu^{63}(\gamma,n)Cu^{62}$ reaction.

Table 2.

Comparison of cross section results for the $Cu^{63}(\gamma,n)Cu^{62}$ and $C^{12}(\gamma,n)C^{11}$ reactions.

Reaction	Threshold (Mev)	Energy at peak cross section (Mev)	Width at half maximum (Mev)	Reference
$Cu^{63}(\gamma,n)Cu^{62}$	10-12	22	3	a
	10.9	17.5	6	b
	10.9	17.5	5.75	c
	10.6	17	6.5	d
	-	18±1	6	e
$C^{12}(\gamma,n)C^{11}$	16-18	30	10	a
	18.7	22.4 0.5	4.25	f
	17.5	20	3.50	d
	-	30±4	14±3	e

[a]Reference 11.

[b]Reference 12.

[c]Reference 16.

[d]Results of this paper.

[e]Reference 24.

[f]Reference 14.

3. $C^{12}(\gamma,n)C^{11}$ cross section results.

The threshold for this reaction was found to be at 17.5 Mev, as compared to the value of 18.7 ± 0.1 Mev given by McElhinney et al. (45). This discrepancy is caused partly by the fact that the synchrotron is only calibrated (by measurements of its magnetic field and of the equilibrium orbit) to an accuracy of about 2 or 3 percent; in addition, the activity near the threshold was low making the results in this region subject to somewhat large statistical errors.

The cross section for this reaction was found to have a maximum value at 20 Mev and to approach zero at around 27 Mev. (see Fig. 12). For a comparison with other results see Table 2.

Here, calculations using this cross section were performed to obtain activation results to check against the experimental values at $E_0 - \mu = 39.5$ Mev and 59.5 Mev. From Fig. 9 it is seen that the agreement is very good.

Both cross sections exhibited an abrupt increase in cross section around their thresholds. McElhinney et al. (45) have indicated this sudden increase in cross section is to be expected. It is pointed out in their paper that, due to the effective thickness of a target, the intensity of any isochromat in the region of the maximum photon energy may be expected to increase with the energy below

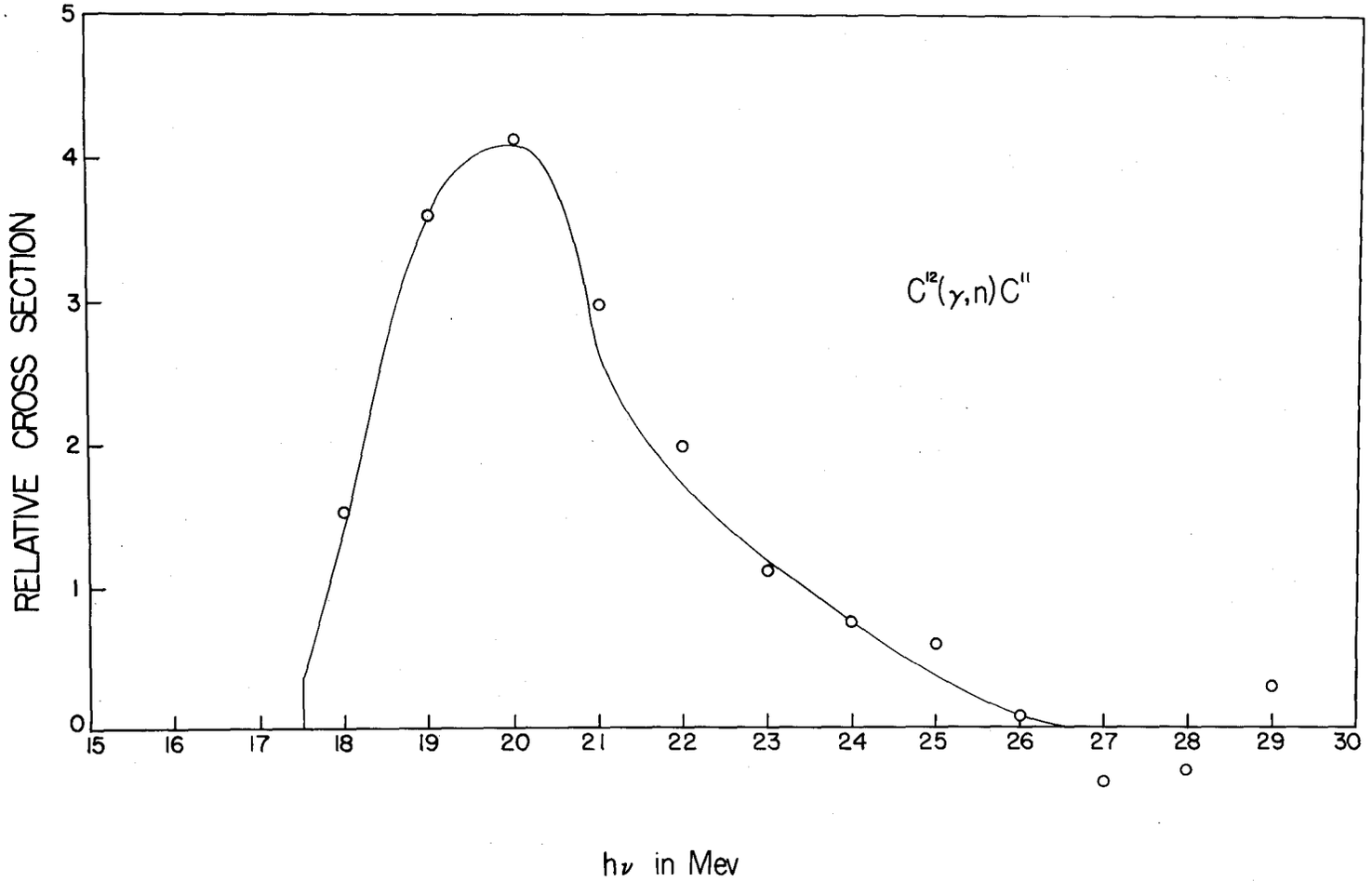

Fig. 12. Relative cross section for the $C^{12}(\gamma,n)C^{11}$ reaction.

the maximum. Under these conditions, to account for the quadratic variation of the activation function around the threshold, the cross section would have to rise abruptly to rather large values.

The effect, on the above cross section results, of a small tail on the silver cross section should be considered here. The presence of this tail would introduce no appreciable change in the adjusted photon distribution results below about 20 Mev, but in the region from 20 Mev up to 60 Mev all of the photon distribution curves would be decreased in amplitude slightly. Thus, in order to produce the same activation results in this region, since the number of photons would be smaller, the cross section would be larger, resulting in small tails on both the $Cu^{63}(\gamma,n)Cu^{62}$ and $C^{12}(\gamma,n)C^{11}$ cross sections.

III. DISCUSSION

A. Evaluation of Experiment

The comparison of cross section data in Table 2 indicates there is very good agreement between the results of this paper and those of Katz et al. and Diven and Almy. Because the results were arrived at by two different methods, it may be concluded that if one method is correct then the other is also correct. There is only fair agreement of the results obtained here with the work of Sagane, and Baldwin and Klaiber.

It is believed that the cross section shapes obtained here are as accurate as those of Katz et al. and Diven and Almy. These results, in turn, are believed to be more accurate than those of Sagane, and Baldwin and Klaiber, who assume a rectangular bremsstrahlung intensity distribution and obtain the cross section by a simple differentiation of the corrected yield curve. Besides the assumption of a rectangular intensity distribution, Baldwin and Klaiber make a calculation of the response of their ion chamber monitor to this distribution based upon simple assumptions which are least accurate in the energy region where the cross sections occur.

With the exception of Sagane's method of simultaneous activation which requires no special apparatus, the method

of obtaining activation data as presented in this paper would appear to be more convenient than the other methods. It is also free of the troublesome necessity of theoretically calculating the response of an ion chamber to the bremsstrahlung spectrum. In addition, no consideration of the change in intensity-angle distribution with change in electron energy is required. This problem would have to be considered in any response calculation concerning an ion chamber.

Although the method of simultaneous activation due to Sagane has the advantage that no special apparatus is required, investigations are limited to cross sections which occur in energy well above the resonant peak of the monitor cross section, unless an activation curve for the monitor reaction is determined in some manner. This limitation does not apply to the technique described here. The main advantage of this technique over the method of simultaneous activation, however, is that the half-life activity of the monitor sample is the same as that of the test sample. This means that the effect of intensity changes is eliminated more completely than with a monitor sample whose half-life activity is only approximately that of the test sample.

The main criticism against the new method, it seems, is the inaccuracy in the adjusted photon distribution due

to the error in the silver cross section. In view of the good agreement with the work previously referred to, however, and because the results are completely consistent in themselves, it is felt that this error is not appreciable. It should be pointed out here that the investigation of cross sections which lie beyond $E_o - \mu = 30$ Mev would be free somewhat of this error, since at higher energies the adjustment of the photon distribution is almost independent of the cross section shape for the $Ag^{107}(\gamma,n)Ag^{106}$ reaction.

The criticism mentioned above could be removed by using a pair spectrometer of good resolving power, instead of the silver reaction, to adjust the photon distribution. It would be necessary to use the oscillator and to follow the same procedure as that used in obtaining an activation curve, except that electron pairs would be counted instead of measuring radioactivity. The results, when plotted, would lead immediately to the adjusted photon distribution. If a sufficiently large number of pairs were observed, the final results could be quite accurate. Also, with the pair spectrometer, reliable cross section curves for a few suitable reactions could be obtained. These could subsequently serve as trustworthy "secondary standards" for work on other reactions with the aid of the convenient method presented in this paper.

Another criticism of the new method, and a valid one for any method based upon the measurement of radioactivity, is that any reactions which result in activities of very short or very long half-life cannot be studied conveniently. In such cases, however, the reactions may be studied by observing the particles which come off when the reaction occurs.

Summarizing briefly, a new method of cross section measurement has been presented which has certain definite advantages over other methods, but leads to results which are no more accurate than the best results of the other methods. Better accuracy could be obtained by the proper use of a well designed pair spectrometer to determine the adjusted photon distribution.

B. Comparison of Theoretical and Experimental Adjusted Photon Distributions

Because of the method of monitoring used in the experiment, it might be supposed that the required photon distribution is the integrated one of Bethe and Heitler (2) (corresponding to an electron beam of constant intensity), multiplied by the fraction of the total photon intensity which falls on the sample being irradiated. This fraction can be calculated from the intensity-angle distribution results due to Schiff (58). The application of this

fraction to the integrated distribution gives the theoretical photon distribution curve shown in Fig. 13.

The results of intensity-angle distribution experiments performed here were used to calculate an experimental curve for comparison with the theoretical one. The intensity distributions were obtained by irradiating copper samples ($\frac{1}{2}$ inch × $\frac{1}{2}$ inch × 0.045 inch) mounted parallel to the synchrotron beam and distributed along the arc of a circle about 7 feet from the synchrotron target. After irradiation at a particular electron energy, the activity due to the $Cu^{63}(\gamma,n)Cu^{62}$ reaction was obtained for each sample and the respective saturation activities then calculated. A plot of the results gave an intensity-angle distribution at the particular electron energy. The analysis, however, was complicated by the presence of small secondary intensity distributions to either side of the main one, which made it difficult to determine the zero point of the main distribution. A small error in locating this point has considerable effect on the calculation of the fraction of the total intensity which falls on the sample.

The intensity distributions were compared with those of Schiff (58) over the range where the effect of the secondary distributions is inappreciable (0^{o} to 5^{o} from the center-line of the main beam). The agreement was very good at high electron energies around 50-60 Mev but the agreement was poor at lower energies, the experimental

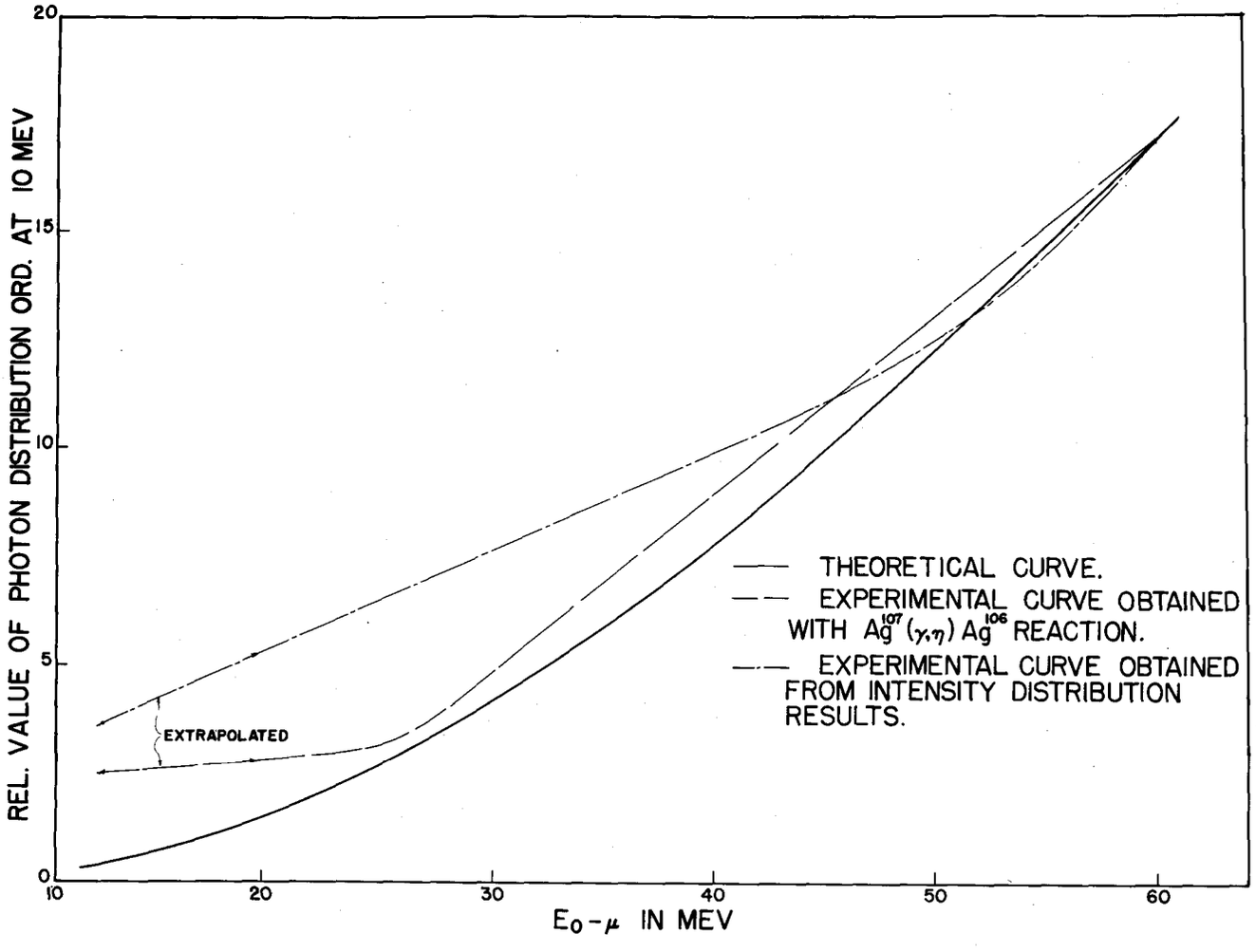

Fig. 13. Comparison of the theoretical and experimental adjusted photon distributions.

distributions being narrower than the theoretical distribution. The experimental curve obtained from these results is shown in Fig. 13, normalized to agree at 60 Mev with the theoretical curve. The difference can be attributed to the narrowness at the lower energies of the experimentally obtained intensity-angle distributions, as well as to the errors introduced by the inaccuracy in the location of the zero point.

For comparison, the experimental curve obtained by means of the silver reaction is also shown in Fig. 13. The disagreement of this curve with theory can be attributed partly to the narrowness of the experimental intensity-angle distribution mentioned above. In addition, such things as multiple traversals of the target by electrons and the loss of some electrons in the orbit could be responsible for part of the disagreement.

VIII. LITERATURE CITED

(1) J. Chadwick and M. Goldhaber, Proc. Roy. Soc. (London) A151, 479 (1935).

(2) H. Bethe and W. Heitler, Proc. Roy. Soc. (London) A146, 83 (1934).

(3) H. W. Koch and R. Carter, Phys. Rev. 77, 165 (1950).

(4) Richard H. Stokes, Cloud chamber measurement of electron pairs for determination of synchrotron spectra. Unpublished Ph.D. thesis. Ames, Iowa, Iowa State College Library. 1951. (To be published in condensed form in the Physical Review).

(5) J. W. DeWire and L. A. Beach, Phys. Rev. 83, 476 (1951).

(6) W. Bothe and W. Gentner, Zeit. f. Physik 106, 236 (1937); 112, 45 (1939).

(7) O. Huber, O. Lienhard, P. Scherrer, and H. Wäffler, Helv. Phys. Acta 15, 312 (1942); 16, 33 (1943); 16, 226 (1943); 17, 134 (1944); 17, 251 (1944); 17, 195 (1945).

(8) O. Hirzel and H. Wäffler, Helv. Phys. Acta 21, 200 (1948).

(9) B. Russel, D. Sachs, A. Wattenberg, and R. Fields, Phys. Rev. 73, 545 (1948).

(10) H. Wäffler and S. Younis, Helv. Phys. Acta 22, 414 (1949).

(11) G. C. Baldwin and G. S. Klaiber, Phys. Rev. 73, 1156 (1948).

(12) L. Katz, H. E. Johns, R. A. Douglas, and R. N. H. Haslam, Phys. Rev. 80, 1062 (1950).

(13) L. Katz and A. S. Penfold, Phys. Rev. 81, 815 (1951).

(14) R. N. H. Haslam, H. E. Johns and R. J. Horsley, Phys. Rev. 82, 270 (1951).

(15) L. Katz, H. E. Johns, R. N. H. Haslam, R. A. Douglas, and R. G. Baker, Phys. Rev. 82, 271 (1951).

(16) B. C. Diven and G. M. Almy, Phys. Rev. 80, 407 (1950).

(17) M. Toms and W. E. Stephens, Phys. Rev. 82, 709 (1951).

(18) A. K. Mann and J. Halpern, Phys. Rev. 80, 470 (1950); 81, 318 (1951).

(19) E. R. Gaertner and M. L. Yeater, Phys. Rev. 77, 714 (1950); 82, 461 (1951).

(20) E. R. Gaertner and M. L. Yeater, Phys. Rev. 83, 146 (1951).

(21) H. W. Koch, J. McElhinney, and J. Cunningham, Phys. Rev. 81, 318 (1951).

(22) K. Strauch, Phys. Rev. 81, 973 (1951).

(23) L. Eyges, Phys. Rev. 81, 981 (1951).

(24) R. Sagane, Phys. Rev. 83, 174 (1951).

(25) M. L. Perlmen and G. Friedlander, Phys. Rev. 74, 442 (1948).

(26) M. Goldhaber and E. Teller, Phys. Rev. 74, 1046 (1948).

(27) H. Steinwedel, J. Jensen, and P. Jensen, Phys. Rev. 79, 1019 (1950).

(28) J. S. Levinger and H. A. Bethe, Phys. Rev. 78, 115 (1950).

(29) M. L. Wiedenbeck, Phys. Rev. 69, 235 (1946).

(30) M. L. Perlman and G. Friedlander, Phys. Rev. 72, 1272 (1947).

(31) M. L. Perlman, Phys. Rev. 75, 988 (1949).

(32) H. Wäffler and O. Hirzel, Helv. Phys. Acta 20, 373 (1947).

(33) L. I. Schiff, Phys. Rev. 73, 1311 (1948).

(34) V. F. Weisskopf and D. H. Ewing, Phys. Rev. 57, 472 (1940).

(35) D. Mock, R. R. Waddel, L. W. Fagg, and R. A. Tobin, Phys. Rev. 74, 1536 (1948).

(36) R. B. McDaniel, R. L. Walker and M. B. Stearns, Phys. Rev. 80, 807 (1950).

(37) G. A. Price and D. W. Kerst, Phys. Rev. 77, 806 (1950).

(38) G. C. Baldwin and F. R. Elder, Phys. Rev. 78, 76 (1950).

(39) A. G. W. Cameron, Phys. Rev. 82, 272 (1951).

(40) N. Sugerman and R. Peters, Phys. Rev. 81, 951 (1951).

(41) K. M. Terwilliger, L. W. Jones, and W. N. Jarmie, Phys. Rev. 82, 820 (1951).

(42) A. K. Mann and J. Halpern, Phys. Rev. 82, 733 (1951).

(43) P. R. Byerly, Jr. and W. E. Stephens, Phys. Rev. 83, 54 (1951).

(44) G. C. Baldwin and H. W. Koch, Phys. Rev. 67, 1 (1945).

(45) J. McElhinney, A. O. Hanson, R. A. Becker, R. B. Duffield, and B. C. Diven, Phys. Rev. 75, 542 (1949).

(46) A. O. Hanson, R. B. Duffield, J. D. Knight, B. C. Diven, and H. Palevsky, Phys. Rev. 76, 578 (1949).

(47) W. E. Ogle and R. E. England, Phys. Rev. 78, 63 (1950).

(48) W. E. Ogle, L. J. Brown and A. N. Carson, Phys. Rev. 78, 63 (1950).

(49) J. McElhinney and W. E. Ogle, Phys. Rev. 78, 63 (1950).

(50) R. C. Mobley and R. A. Laubenstein, Phys. Rev. 80, 309 (1950).

(51) R. W. Parsons and C. H. Collie, Proc. Phys. Soc. (London) A63, 839 (1950).

(52) R. Sher, J. Halpern and W. E. Stephens, Phys. Rev. 81, 154 (1951).

(53) H. L. Poss, Phys. Rev. 79, 539 (1950).

(54) C. Levinthal and A. Silverman, Phys. Rev. 82, 822 (1951).

(55) J. S. Levinger and H. A. Bethe, Phys. Rev. 78, 115 (1950).

(56) E. D. Courant, Phys. Rev. 82, 703 (1951).

(57) L. I. Schiff, Phys. Rev. 70, 87 (1946).

(58) A. G. W. Cameron and L. Katz, Phys. Rev. 83, 892 (1951).

IX. ACKNOWLEDGEMENTS

It is a sincere pleasure to acknowledge the generous cooperation received during the course of the experiment from Dr. L. Jackson Laslett, who originally suggested the problem.

Appreciation is also extended to Mr. Don Steward for his assistance in taking some of the activation data, to Mr. Steward and Mr. Phillip Phipps for aiding in the preparation of the table of photon values, and to Mr. Harold Austrheim for many helpful suggestions made in regard to the construction of the apparatus.